

BAŞKENT ÜNİVERSİTESİ
FEN BİLİMLERİ ENSTİTÜSÜ

136757

HÜCRESEL RADYO SİSTEMLERİNİN
SÖNÜMLÜ VE İLİNTİLİ GÖLGELEMELİ ORTAMLARDAKİ
BAŞARIM ANALİZİ

(PERFORMANCE ANALYSIS OF CELLULAR RADIO SYSTEMS IN FADING AND
CORRELATED SHADOWING ENVIRONMENTS)

İbrahim Baran USLU

YÜKSEK LİSANS TEZİ

ANKARA

OCAK, 2003

136757

T.C. YÜKSEKÖĞRETİM KURULU
DOKÜMANTASYON MERKEZİ

BAŞKENT ÜNİVERSİTESİ
FEN BİLİMLERİ ENSTİTÜSÜ

PERFORMANCE ANALYSIS OF CELLULAR RADIO SYSTEMS IN
FADING AND CORRELATED SHADOWING ENVIRONMENTS

İbrahim Baran USLU

ELEKTRİK-ELEKTRONİK MÜHENDİSLİĞİ ANABİLİM DALI

YÜKSEK LİSANS TEZİ

Bu tez, 27/ 01/ 2003 tarihinde aşağıda üye adları yazılı jüri tarafından kabul edilmiştir.

Ünvan

Adı Soyadı

İmza

Prof. Dr.

Turhan ÇİFTÇİBAŞI



Yrd. Doç. Dr.

Aysel ŞAFAK (Danışman)



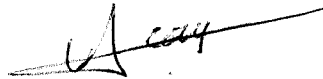
Yrd. Doç. Dr.

Atif ÇAY



Onay

31 / 01 / 2003



Fen Bilimleri Enstitüsü Müdürü
Prof. Dr. Hüseyin AKÇAY

DEDICATION and ACKNOWLEDGEMENTS

This thesis work is dedicated to the professor who taught me *'the rule of survival'*.

First of all I'd like to thank to my supervisor Asst. Prof. Dr. Aysel ŞAFAK for her encouraging, motivating and helpful supervision. Without her mothership I wouldn't success.

My family was always with me with their love and all study long.
Thanks and love to them.

I also would like to thank to my research assistant colleagues for their valuable helps at the completing stage.

My last but not least acknowledgement is for Mr. Erdi ÇINAR, system administrator of Başkent University, for his valuable friendship.

OUTLINE

ÖZ

ABSTRACT

TABLE OF CONTENTS

LIST OF FIGURES

LIST OF SYMBOLS and ACRONYMS

1. INTRODUCTION
2. PROPAGATION ASPECTS OF CELLULAR MOBILE RADIO SYSTEMS
3. PERFORMANCE IMPROVEMENT
4. IMPROVING COVERAGE AND CAPACITY IN CELLULAR SYSTEMS
5. SMART ANTENNAS
6. ADAPTIVE BEAMFORMING IN MOBILE COMMUNICATIONS
7. RESULTS AND CONCLUSIONS
8. REFERENCES
9. ÖZGEÇMİŞ

ÖZ

HÜCRESEL RADYO SİSTEMLERİNİN SÖNÜMLÜ VE İLİNTİLİ GÖLGELEMELİ ORTAMLARDAKİ BAŞARIM ANALİZİ

İbrahim Baran USLU

YÜKSEK LİSANS TEZİ
ELEKTRİK-ELEKTRONİK MÜHENDİSLİĞİ ANABİLİM DALI

Danışman: Yrd. Doç. Dr. Aysel ŞAFAK
Ocak 2003

Hücresel sistemlerin başarımı, çok-yollu sönümlü, ilintili gölgelemeli ve Gauss dağılımlı toplamsal beyaz gürültülü ortamlarda, FSK, PSK ve DPSK modülasyon metodları kullanılarak, heryönlü, yönlü ve adaptif antenler için incelenmiştir. Hem istenen sinyalin, hem de girişimci sinyallerin kanaldaki düzgün sönümlenmenin ve gölgelenmenin etkisi altında olduğu kabul edilmiştir. Sistemin başarımı ortak-kanal girişim olasılığı, bit hata oranı ve spektrum verimliliği cinsinden incelenmiştir. Hücresel sistemlerin başarımını değerlendirmek için yeni formüller geliştirilmiştir. Bit enerjisi / gürültü güç yoğunluğu (E_b / N_0), işaret-girişimci güç oranı (ξ_d / ξ_u), frekans tekrar kullanım uzaklığı (R_u), petek büyüklüğü (C), gölgelenmenin standart sapması (σ), sinyaller arasındaki ilinti katsayısı (ρ), girişimci sayısı (n), Rician faktörü (K), kanal kullanım verimliliği (η), hücre başına toplam kanal sayısı (M), anten eleman sayısı (μ) ve trafik parametreleri gibi bazı sistem parametrelerinin hücresel sistemlerin başarımı üzerindeki etkileri araştırılmıştır. Bütün durumlarda adaptif dizi antenlerin, heryönlü ve yönlü anten sistemlerinden daha iyi performans gösterdiği, ortak-kanal girişim olasılığını ve bit hata oranını önemli ölçüde düşürerek sistemin spektrum verimliliğini ve başarımını arttırdığı gözlenmiştir.

Bilgisayar simülasyonları ile, gezgin iletişim sistemlerinde adaptif anten kullanımının sistemin spektrum verimliliği ve başarımındaki yararları üzerinde çalışmalar yapıldı. Sonuçlar, adaptif anten dizilerinin hücresel sistemlerin spektrum verimliliğini ve başarımını belirgin ölçüde arttırdığını göstermektedir.

Anahtar Kelimeler:

Hücre, hücresel gezgin iletişim sistemi, frekans tekrar kullanımı, ortak-kanal girişimi, spektrum verimliliği, sektörleme, sönümlenme, ilintili gölgelenme, adaptif demetleme, LMS algoritması.

ABSTRACT

PERFORMANCE ANALYSIS OF CELLULAR RADIO SYSTEMS IN FADING AND CORRELATED SHADOWING ENVIRONMENTS

İbrahim Baran USLU

M.Sc. Thesis

DEPARTMENT OF ELECTRICAL-ELECTRONICS ENGINEERING

Supervisor: Asst. Prof. Dr. Aysel ŞAFAK

January, 2003

The performance of cellular radio systems was investigated in multipath fading, correlated shadowing and additive white Gaussian noise environments for FSK, PSK and DPSK modulation with omnidirectional, directional and adaptive antennas. Both desired and interfering signals are assumed to be under flat fading and correlated shadowing in the channel. System performance is evaluated in terms of probability of co-channel interference, bit error rate and spectrum efficiency. Formulas for evaluating the performance of cellular radio systems are presented. The effects of bit energy to noise power ratio (E_b/N_0), signal-to-noise power ratio (ξ_d/ξ_u), frequency reuse distance (R_u), cluster size (C), shadow spread (σ), correlation coefficient between the signals (ρ), number of interferers (n), Rician factor (K), channel usage efficiency (η), total number of channels per cell (M), number of antenna elements (μ) and some traffic parameters, on the performance of cellular systems were studied.

Computer simulations are carried out for evaluating the benefits of using adaptive antennas in mobile communications in terms of spectrum efficiency and system performance. Results show that application of adaptive antenna arrays increase the spectrum efficiency and the performance of the cellular systems.

Keywords:

Cell, cellular mobile radio system, frequency reuse, co-channel interference, spectral efficiency, sectorization, fading, correlated shadowing, adaptive beamforming, LMS algorithm.

TABLE OF CONTENTS

DEDICATION and ACKNOWLEDGEMENTS	iii
OUTLINE	iv
ÖZ	v
ABSTRACT	vi
LIST OF FIGURES	ix
LIST OF SYMBOLS and ACRONYMS	xi

CHAPTER-1

INTRODUCTION.....	1
1.1 MOBILE RADIO SYSTEMS	1
1.2 CELLULAR RADIO SYSTEMS.....	2
1.2.1 Coverage Layout	3
1.2.2 Cluster Size.....	3
1.2.3 Normalized Frequency Reuse Distance	5
1.2.4 Cell Splitting.....	6
1.2.5 Spectrum Efficiency	7
1.2.6 System Design Fundamentals	9
1.3 MULTIPLE ACCESS.....	10

CHAPTER-2

PROPAGATION ASPECTS OF CELLULAR MOBILE RADIO SYSTEMS.....	13
2.1 MOBILE RADIO PROPAGATION.....	13
2.2 SMALL-SCALE FADING AND MULTIPATH PROPAGATION.....	14
2.3 LARGE-SCALE FADING AND LOG-NORMAL SHADOWING.....	15
2.4 LARGE-SCALE PATH LOSS.....	16

CHAPTER-3

PERFORMANCE IMPROVEMENT	18
3.1 THE MEASURE OF PERFORMANCE.....	18
3.2 PROBABILITY OF CO-CHANNEL INTERFERENCE	18
3.3 PROBABILITY OF A BIT ERROR.....	22

CHAPTER-4

IMPROVING COVERAGE AND CAPACITY IN CELLULAR SYSTEMS	25
4.1 CELL SPLITTING	25
4.2 SECTORIZATION	27
4.2.1 Design of an Omnidirectional Antenna System	28
4.2.2 Design of a Directional Antenna System	29
4.2.2.1 Directional Antennas in C=7 Cell Patterns	30
a) Three-sector case	30
b) Six-sector case	31
4.2.2.2 Directional Antennas in C=4 Cell Patterns	32
a) Three-sector case	32
b) Six-sector case	32
4.3 RESULTS AND CONCLUSIONS	33

CHAPTER 5

SMART ANTENNAS.....	39
5.1 SWITCHED-BEAM SYSTEMS.....	40
5.2 ADAPTIVE ANTENNA SYSTEMS.....	41
5.3 RESULTS AND CONCLUSIONS	43

CHAPTER 6

ADAPTIVE BEAMFORMING IN MOBILE COMMUNICATIONS.....	47
6.1 OPERATION OF ADAPTIVE ANTENNA ARRAYS.....	47
6.2 REDUCTION OF CO-CHANNEL INTERFERENCE USING ADAPTIVE ANTENNAS.....	49
6.3 RESULTS AND CONCLUSIONS.....	51

CHAPTER 7

RESULTS AND CONCLUSIONS.....	55
-------------------------------------	-----------

REFERENCES.....	57
------------------------	-----------

ÖZGEÇMİŞ.....	59
----------------------	-----------

LIST OF FIGURES

Figure 1.1 Idealized hexagonal cell layout and frequency reuse pattern with a cluster of $C=7$ cells ($i=2, j=1$).....	4
Figure 1.2 Frequency reuse distance in an idealized hexagonal cell pattern with a cluster of $C=7$ cells.....	5
Figure 1.3 Variation of normalized frequency reuse distance and spectrum efficiency as a function of the cluster size.....	8
Figure 1.4 120° sectorized cell pattern.....	12
Figure 1.5 Independent steering of the users simultaneously by an adaptive antenna	12
Figure 2.1 Typical variation of the received signal power with combined fading and shadowing	14
Figure 2.2 Rayleigh, Rice and log-normal pdf's.....	17
Figure 4.1 Cell Splitting.....	26
Figure 4.2 Sectors in 120° and 60° sectorization.....	27
Figure 4.3 First and second tiers in the cellular system.....	28
Figure 4.4 Co-channel interference, worst case in <i>omnidirectional</i> antenna system...29	29
Figure 4.5 Interferers in 120° and 60° sectoring.....	30
Figure 4.6 Co-channel interference, worst case in 120° sectoring.....	31
Figure 4.7 Co-channel interference, worst case in 60° sectoring.....	32
Figure 4.8 Effect of R_u , K_d , ρ and E_b/N_0 on BER for <i>omnidirectional</i> antenna systems under shadowing and Rician/Rayleigh fading.....	33
Figure 4.9 Effect of R_u , K_d , ρ and E_b/N_0 on BER for 120° <i>directional</i> antenna systems under shadowing and Rician/Rayleigh fading.....	34
Figure 4.10 Effect of R_u , K_d , ρ and E_b/N_0 on BER for 60° <i>directional</i> antenna systems under shadowing and Rician/Rayleigh fading.....	35
Figure 4.11 Effect of K_d and traffic per channel (α_c) on spectral efficiency for <i>omnidirectional</i> antenna systems under shadowing and Rician/Rayleigh fading.....	36

Figure 4.12 Effect of K_d and correlation coefficient (ρ) on the spectrum efficiency for <i>omnidirectional</i> antenna systems under shadowing and Rician/Rayleigh fading.....	37
Figure 4.13 Effect of K_d and correlation coefficient (ρ) on the spectrum efficiency for <i>120° directional</i> antenna systems under shadowing and Rician/Rayleigh fading.....	38
Figure 5.1a Switched-beam system.....	39
Figure 5.1b Adaptive antenna.....	39
Figure 5.2 A rosette of directional beams for a smart antenna.....	40
Figure 5.3 Uniformly spaced (d), 7-element linear adaptive array.....	41
Figure 5.4a Radiation pattern of the uniformly spaced 10-element linear adaptive antenna array with 2 interferers.....	44
Figure 5.4b Squared error of the uniformly spaced 10-element linear adaptive array for the 2-interferer case.....	44
Figure 5.5a Radiation pattern of the uniformly spaced 10-element linear adaptive antenna array with 4 interferers.....	44
Figure 5.5b Squared error of the uniformly spaced 10-element linear adaptive array for the 4-interferer case.....	44
Figure 5.6a Radiation pattern of the uniformly spaced 10-element linear adaptive antenna array with 6 interferers.....	46
Figure 5.6b Squared error of the uniformly spaced 10-element linear adaptive array for the 6-interferer case.....	46
Figure 5.7a Radiation pattern of the uniformly spaced 10-element linear adaptive antenna array with 6 interferers.....	46
Figure 5.7b Squared error of the uniformly spaced 10-element linear adaptive array for the 6-interferer case.....	46
Figure 6.1 Adaptive antenna array.....	48
Figure 6.2 Effect of the number of antenna elements (μ) on the co-channel interference probability with: 1-interferer, $\sigma = 4\text{dB}$, $K = 6\text{dB}$, $\rho = 0$	52
Figure 6.3 Effect of the number of antenna elements (μ) on the co-channel interference probability with: 6-interferer, $\sigma = 4\text{dB}$, $K_d = 6\text{dB}$, $\rho = 0$	52

Figure 6.4 Effect of the number of antenna elements (μ) on BER with NCDPSK modulation.....53

Figure 6.5 Effect of the number of antenna elements (μ) on BER with NCFSK modulation.....53

Figure 6.6 Effect of the number of antenna elements (μ) on BER with uncorrelated interferers, $\rho = 0$54

Figure 6.7 Effect of the number of antenna elements (μ) on BER with correlated interferers, $\rho = 1$54



LIST OF SYMBOLS

a :	: path loss exponent for $d \ll g$
a_c :	: traffic carried per channel (erlang / channel)
A :	: offered traffic per cell (erlang / cell)
A_c :	: traffic carried by a cell (erlang / cell)
b :	: additional path loss exponent for $d \gg g$
B :	: blocking probability
C :	: cluster size
d :	: distance between the transmitter and the receiver
D :	: distance between two nearest co-channel cells
E_s :	: spectrum efficiency
E_b/N_0 :	: the ratio of the energy per bit to the noise spectral density
$f_{P_d, P_u} (P_d, P_u)$:	: joint pdf of the instantaneous powers of the desired and the sum of interfering signals
$F(CI)$:	: total PCI (see the list of acronyms)
$F(CI n)$:	: PCI conditioned on the number of active co-channel interferers
g :	: turning point of the path loss curve
$I_0(.)$:	: modified Bessel function of the first kind and zero order
K_d :	: Rice factor of the desired signal
K_i :	: Rice factor of the i^{th} interfering signal
M :	: number of available channels per cell
m_d :	: logarithmic mean power of the desired signal
m_u :	: logarithmic mean power of the undesired signal
μ :	: number of antenna elements
n :	: basic propagation path-loss exponent
N_c :	: number of available channels per cluster
N_T :	: total number of available channels
P_d :	: received instantaneous power of the desired signal
$P_n(e n)$:	: conditional BER in the presence of n active interferers
P_{od} :	: local mean power of the desired signal
P_{oi} :	: local mean power of the i^{th} interferer
P_{ou} :	: local mean power of the sum of interfering signals

P_r	: received power
P_t	: transmitted power
P_u	: received instantanenuous power of the sum of interfering signals
R	: cell radius
R_u	: normalized frequency reuse distance
S_c	: area of a cell.
W	: bandwidth per channel
$\phi_n(t)$: n^{th} path phase
σ_d	: shadow spread of the desired signal
σ_u	: shadow spread of the undesired signal
ξ_d	: area mean signal power of the desired signal
ξ_u	: area mean signal power of the sum of interfering signals
$\rho_{i,j}$: correlation coefficient between the i^{th} and j^{th} signal
α	: co-channel protection ratio

LIST OF ACRONYMS

AWGN	: Additive White Gaussian Noise
BER	: Bit Error Rate
NCDPSK	: Non-Coherent Differential Phase Shift Keying
NCFSK	: Non-Coherent Frequency Shift Keying
PCI	: Prabability of Co-channel Interference
pdf	: probability density function
ULA	: Uniform Linear Array
AOA	: Angle of Arrival

CHAPTER-1

INTRODUCTION

The 1990' s have been described as the decade of wireless telecommunications. The evolution of telecommunications from the wired phone to personal communications services, is resulting in the availability of wireless services, which were not previously considered practical. In providing different types of wireless services, such as fixed, mobile, outdoor, indoor, and satellite communications, the wireless communications industry is experiencing an explosive growth.

1.1 MOBILE RADIO SYSTEMS

Most people are familiar with a number of mobile radio communication systems used in everyday life. Garage door openers, remote controllers for home entertainment equipment, cordless telephones, hand-held walkie-talkies, pagers and cellular telephones are all examples of mobile radio communication systems. However, the cost, complexity, performance, and types of services offered by each of these mobile systems are vastly different.

The expanding need and explosive growth in wireless communications have led to the development of cellular mobile radio systems. One of many reasons for developing a cellular radio system is the operational limitations of conventional mobile systems such as limited service capability without hand-off and locating, poor service performance and insufficient frequency spectrum utilization.

A conventional mobile system is designed by selecting channels from a specific frequency allocation for use in autonomous geographic regions. The communications coverage area of these regions is planned to be as large as possible, which means that

the transmitted power should be as high as the specifications allow. Thus, the conventional system does not utilize the spectrum efficiently since each channel can only serve one customer at a time in the whole region.

As the number of users is increased, the available frequency spectrum becomes unable to handle the increased traffic, and consequently a need for *frequency reuse* arises. Instead of covering an entire service area from one base station with high transmitter power, the service area is then split into many small sub-areas called *cells*, each of which is served by a different base station of moderate transmitter power. One particular group of channels is repeatedly used in co-channel cells, which are separated by a certain *frequency reuse distance* so as to keep the co-channel interference to an acceptable level.

Cellular radio thus differs from the conventional radio in two important aspects: frequency reuse and cell splitting. Frequency reuse offers increased system capacity while smaller cell sizes lead to increased service quality, but at the expense of increased complexity of network infrastructure and operations. The trade-offs between the equipment cost, network complexity and the quality of service determine the shape and size of the cellular network.

1.2 CELLULAR RADIO SYSTEMS

The need for serving a very large number of customers in a given service area, within a limited frequency band and with constraints on cost, has spurred the evolution of the cellular concept. A typical cellular radio system consists of three classes of entities: mobile terminals, base stations, and mobile switching centres. A mobile terminal contains a control unit, a transceiver, and an antenna system. Each base station has radio equipment and associated control that can provide connection to any mobile terminal located in its cell. The base stations are interconnected and controlled by a central switch. The mobile switching centre, the central coordinating element for all base stations, contains a cellular processor and a cellular switch.

1.2.1 Coverage Layout

In cellular radio systems, repeated use of regular polygons such as the equilateral triangle, square or regular hexagon can cover a service area with no gaps or overlaps. If they all have the same centre-to-vertex distance, then the hexagon has a substantially larger area. Consequently, to serve a given total coverage area, hexagonal lay-out requires fewer cells, hence fewer base station sites. A cellular system based on hexagonal cells, therefore, costs less than the one with triangular or square cells, all other factors being equal. But in practice, this coverage plan is not that much ideal; because it won't be possible to put the base station in every wanted place and the antenna systems are not perfect in directivity. So there will be some uncovered or overlapped places in coverage.

1.2.2 Cluster Size

In cellular systems, large planar regions can be covered by two dimensional networks of small coverage cells. In this system, the cells form a fixed block or cluster around the reference cell in the centre and around its co-channel cells. In a cellular system, the minimum number of cells per cluster: C , in a cell reuse pattern is a function of the co-channel separation. The number of cells per cluster, referred to as *cluster size* as well, is a parameter of major interest, since in practice this number determines how many different channel sets must be formed out of the total allocated spectrum. If the total number of channels available for our system: N_T , is partitioned into C cells, then each cell will contain $N_s = N_T / C$ channels. If one channel set is used in each cell, the telephone traffic demand in some cell will be maximum that cell's N_s channels. Further growth in traffic within the cell will require a revision of the cell boundaries so that the area formerly regarded as a single cell can now contain several cells and utilize all these cells' channel complements. It is this process which is called cell splitting.

For hexagonal systems, the cluster size: C , is determined by:

$$C = i^2 + ij + j^2 \quad i, j \geq 0 \quad (1.1)$$

The fact that i and j are integers makes geometrically realizable only certain values of the number of cells per cluster, e.g., 1, 3, 4, 7, 9, 12, 13...

$i=2$ and $j=0$ for $C=4$, $i=2$ and $j=1$ for $C=7$, $i=2$ and $j=2$ for $C=12$...

Figure 1.1 shows the layout and frequency reuse pattern for a cluster of seven hexagonal cells with $i=2$ and $j=1$. Note that the co-channel cells, i.e., those cells that use the same frequencies, could be located by moving i cells along any chain of hexagons and turning counter-clockwise 60° and then moving j cells along the chain. The adjacent cells are allocated different frequencies. Between two co-channel cells many equal size cells must be filled with different frequencies in order to provide a continuity of frequency coverage in space so that the mobile terminals can communicate [1].

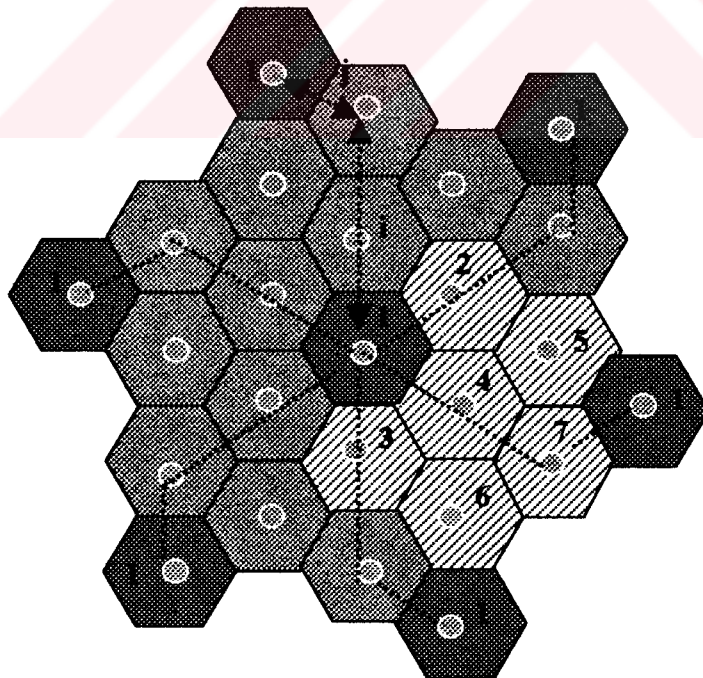


Figure 1.1 Idealized hexagonal cell layout and frequency reuse pattern with a cluster of $C=7$ cells ($i=2, j=1$)

1.2.3 Normalized Frequency Reuse Distance

When customer demand increases, the channels, which are limited in number, have to be repeatedly reused in different areas. This leads to more co-channel cells and increases the system capacity. The minimum separation required between two nearby co-channel cells is based on specifying a maximum tolerable co-channel interference due to transmissions from other co-channel cells. The level and distribution of this interference depend on the frequency reuse pattern, the wave propagation phenomenon and the way in which this has been balanced against systems' cost and overall performance objectives [2].

Let D and R denote the distance between the centres of two closest co-channel cells, and the radius of the circle approximating the standard cell, respectively. See Figure 1.2.

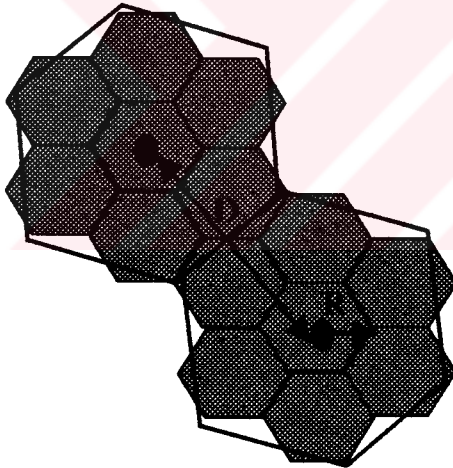


Figure 1.2 Frequency reuse distance in an idealized hexagonal cell pattern with a cluster of $C=7$ cells.

The *frequency reuse distance* normalized by the cell radius: R_u , is defined by:

$$R_u = D / R \quad (1.2)$$

For hexagonal systems, the relationship between the normalized frequency reuse distance: R_u , and the number of cells per cluster: C , required to completely cover any planar area with a fixed assignment plan is simply:

$$R_u = \sqrt{3C} \quad (1.3)$$

Note that, in view of (1.1), R_u is allowed to take only some discrete values, as determined by the integer values of the cluster size.

The minimum distance which allows the same frequency to be reused will depend on many factors, such as the number of co-channel cells in the vicinity of the centre cell, the type of geographic terrain contour, the antenna height, and the transmitted power of each base station. The reduction of the normalized frequency reuse distance would increase the system capacity and the efficiency of spectrum usage.

If all the base stations transmit the same power, then the cluster size, C , increases and the frequency reuse distance: R_u increases. The increased frequency reuse distance reduces the probability of co-channel interference; so a large C is desired. On the other hand, since the total number of allocated channels: N_T is fixed, the number of channels assigned to each of C cells: $N_s = N_T / C$, becomes smaller with increasing C . Therefore, smaller C provides more channels per cell and per base station. Each base station can thus carry more traffic, thereby reducing the total number of base stations needed for a given total load. The challenge is to obtain the smallest value of cluster size and frequency reuse distance which can still meet the system performance requirements. The cluster size, the frequency reuse distance and the number of base stations are limited by several other factors as well, including the economic constraints.

1.2.4 Cell Splitting

The techniques of frequency reuse and cell splitting permit a cellular system to meet the important objectives of serving a very large number of customers in a single coverage area while using a relatively small spectrum allocation. When the call traffic in an area increases, the cell is splitted for denser frequency reuse. Cell splitting helps to meet the objective of matching the spatial density of available channels to the spatial density of demand for channels, since lower-demand areas can be served by larger cells with higher-demand areas being served by smaller cells. By decreasing the area of each

cell, cell splitting allows the system to adjust to a growing spatial traffic demand density (simultaneous calls per unit area) without any increase in the spectrum allocation.

1.2.5 Spectrum Efficiency

The motivation behind implementing a cellular radio system is to use the available frequency spectrum more efficiently. The techniques of frequency reuse and cell splitting permit a cellular radio system to serve a very large number of customers in a single coverage area while occupying a relatively modest frequency band. If the available channels were distributed among smaller cells, the traffic capacity would be greater, while a system with a relatively small capacity would use larger cells. Each channel frequency can then be used for independent calls in several cells, if these are spaced far enough from each other so as to avoid interference. Frequency reuse improves the spectrum efficiency, but at the cost of increasing interference from co-channel cells. The minimum separation required between nearby co-channel cells is based on specifying a maximum tolerable PCI. The level and distribution of PCI depend on the frequency reuse pattern and the wave propagation phenomenon.

Future cellular radio systems must be able to operate in the environment of high spectrum congestion and interference. Since the allocated frequency spectrum is limited, this precious resource must be used as efficiently as possible. Therefore one of the principal objectives for the design of cellular radio systems is to maximize the *spectrum efficiency*, which is a measure of the carried traffic per unit bandwidth and per unit cell area. Spectrum efficiency depends on the cellular structure, modulation technique, channel access scheme, correlation between signals and system performance parameters such as an acceptable PCI or call blocking probability [2,3].

The techniques for increasing the spectrum efficiency include high density reuse of the co-channels, narrow band transmission, demand-assignment multiple access, i.e., efficient time shared use of the available channels, and increasing the channel efficiency. The capacity of cellular systems is directly related to the spectrum efficiency: E_s , which is defined by:

$$E_s = \frac{A_c}{N_s W C S_c} \quad \text{erlang/MHz/km}^2 \quad (1.4)$$

Here, A_c denotes traffic carried by a cell in erlang, N_s is the number of channels per cell, W represents bandwidth per channel in MHz, C is the number of cells per cluster and S_c the area of a cell in km^2 . The traffic carried by a cell is given by:

$$A_c = A (1-B) \quad \text{erlang / cell} \quad (1.5)$$

where A denotes the offered traffic per cell in erlang. The blocking probability: B , is determined using the Erlang-B formula:

$$B = \frac{A^{N_s}}{N_s! \sum_{n=0}^{N_s} \frac{A^n}{n!}} \quad (1.6)$$

Figure 1.3 below shows the variation of the normalized frequency reuse distance and the spectrum efficiency as a function of the cluster size for $A_c = 5$ erlang, $N_s = 10$, $W = 25$ kHz and $S_c = 1 \text{ km}^2$. R_u and E_s values corresponding to the discrete values of C are shown with + and o respectively.

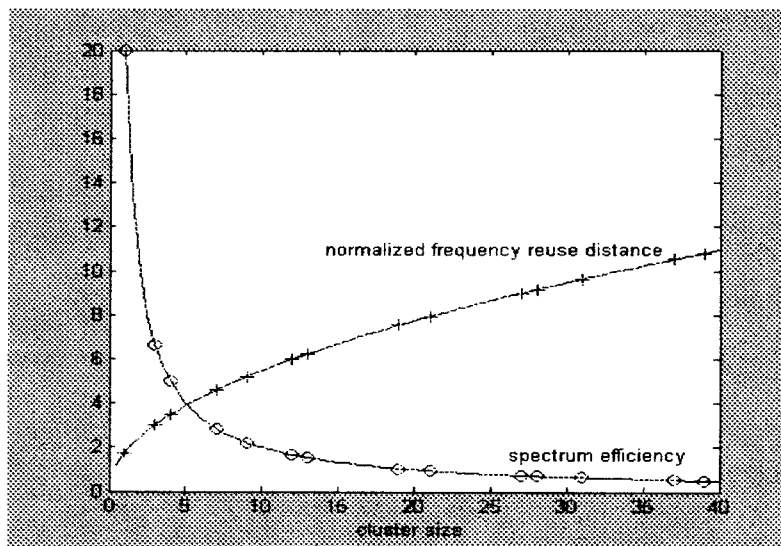


Figure 1.3 Variation of normalized frequency reuse distance and spectrum efficiency as a function of the cluster size

1.2.6 System Design Fundamentals

Main factors in the design of cellular systems include the implementation specifics such as antenna height and type, directivity, system hand-off and control algorithms, siting requirements, channel assignment plan, transmission and system performance parameters such as tolerable co-channel interference level, blocking probability etc. The key geometrical parameters of the cellular layout were chosen primarily to satisfy the objectives of moderate cost, sufficient transmission quality and a large ultimate customer capacity. In many cases, trade-offs must be made among these joint objectives.

Locating and *hand-off* are concepts that come directly from the use of small cells. The act of transferring a mobile terminal from one channel to another as it passes through different cells is called *hand-off* in the USA and *hand-over* in Europe. Each time a mobile terminal enters a different cell associated with a different frequency, a hand-over occurs. The hand-over is an action controlled by the switching centres. Locating is a process for determining whether it would be better, from the point of view of signal quality and potential interference, to transfer an active connection with a mobile terminal to another base station.

When a system is first established, there is normally little frequency reuse since each initial cell is relatively large and the total number of cells needed to span the desired coverage area does not greatly exceed the number of channel sets into which the total allocation is partitioned. The traffic in each cell increases as the number of subscribers increases, so the frequency channels, limited in number, may have to be reused in different areas to raise the capacity of the system. However, more co-channel interference will then occur. In this situation, one must increase the normalized frequency reuse distance and hence the total band required, use directional antennas, or lower the transmit power to create smaller cells where necessary (cell splitting).

In the start-up phase of a system, omnidirectional antennas are used because of their lower investment cost compared to that for the directional systems. In later stages,

directional antennas are employed at the base stations; each cell is divided into, e.g., three or six sectors, each sector being served by an appropriate directional antenna. In comparison with an omnidirectional antenna, a directional antenna can deliver the same signal level to users in its coverage sectors while causing substantially less interference to co-channel cells in other sectors. Therefore, the directional systems can operate with a smaller normalized frequency reuse distance, that is, a closer spacing between co-channel base stations for a given amount of traffic. The omnidirectional systems minimize the initial costs for new systems, whereas the directional systems confine cost in mature systems by reducing the total number of sites required to serve a given offered traffic load.

It is clear that one needs to establish a good model of the system in order to calculate the probability of (unacceptable) co-channel interference (PCI) and relate this, together with the others, to the system design parameters. This allows the designer to see the effects of different choices of parameters and so optimize the system design, including best use of the available frequency bandwidth for a given level of the PCI and traffic load.

1.3 MULTIPLE ACCESS

A higher demand in wireless communications will need higher system capacities. Two direct methods for increasing capacity are enlarging the bandwidth of the existing communication channels or allocating new frequencies to the service. However, since the electromagnetic spectrum is limited and the electromagnetic environment is increasingly becoming congested with a proliferation of unintentional and intentional sources of interference, it may not be feasible in the future to increase system capacity by opening new spectrum space for the wireless communication applications. Therefore efficient use of the frequency resource is critical.

Over the last four decades, engineers have made considerable progress in increasing the capacity of a wireless communication system, especially for digital wireless

communications. Coupling the benefit of source coding and channel coding, digital techniques can significantly reduce either the required transmitter power or the bandwidth of the transmission, or both, and yet achieve better performance or quality than analog systems can. Furthermore, with digital techniques, frequency efficiency can be improved by using multiple access techniques to provide high system capacity. Multiple access is implemented by having the mobile users share the base stations. There are four domains in which sharing can take place.

- 1) bandwidth
- 2) time
- 3) code
- 4) space

In Frequency Division Multiple Access (FDMA), the frequency spectrum is divided into segments that are used by different users. With the arrival of digital techniques, Time Division Multiple Access (TDMA) became a practical access technology. Here each user is allocated the entire transmission resource periodically for a brief period of time. Digital techniques also enable another multiple access method: Code Division Multiple Access (CDMA). CDMA employs spread spectrum modulation (i.e. each user's digital waveform is spread over the entire frequency spectrum that is allocated to all users of the network.) Each of the transmitted signals is modulated with a unique code that identifies the sender. The receiver then uses the appropriate code to detect the signal of choice.

The last form of multiple access is known as Space Division Multiple Access (SDMA). SDMA has been widely used in wireless communications. For example, in a cellular telephone network, where a large geographical coverage is desired and a large number of mobile transceivers must be supported, the region is divided into a large number of cells. In fact this is a primitive form of SDMA, in that communication signals that are transmitted at the same carrier frequency in different cells are separated by a spatial distance to reduce the level of co-channel interference. However communications engineers are realizing that more advanced forms of SDMA are needed. For example 120° sectorial beams at different carrier frequencies can be used within a cell and each sectorial beam can be used to serve the same number of users as are served in the case of ordinary cells, as shown in Figure 1.4. With careful frequency planning, the capacity can be tripled and the carrier-to-interference power ratio (CIR) can also be increased. The ultimate form of SDMA, however, is to use independently

steered high-gain beams at the same carrier frequency to provide service to individual users within a cell. That is communications can be simultaneously carried out between users and the base station. The latest form of SDMA usually employs adaptive antenna arrays. In large measure, adaptive array techniques are dependent on digital beamforming technology for their practical implementation [6].

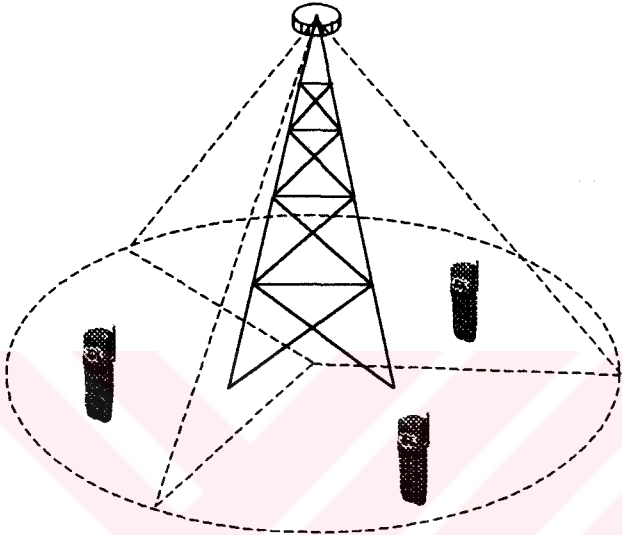


Figure 1.4 120° sectorized cell pattern.

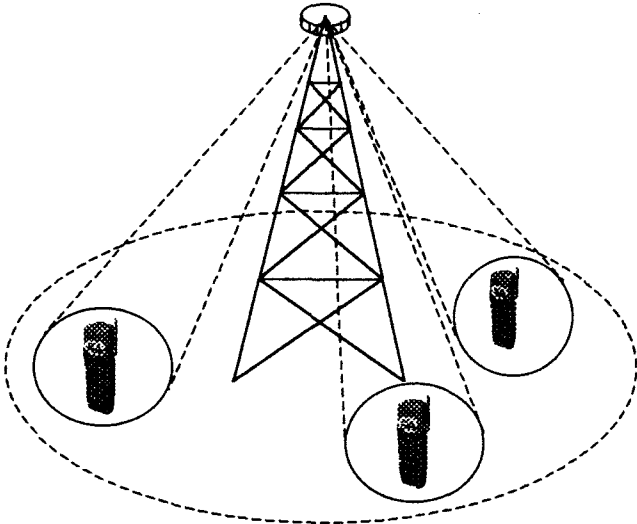


Figure 1.5 Independent steering of the users simultaneously by an adaptive antenna

CHAPTER-2

PROPAGATION ASPECTS OF CELLULAR MOBILE RADIO SYSTEMS

2.1 MOBILE RADIO PROPAGATION

Signal transmission in mobile radio channels presents significantly different problems other than those encountered in wire-line systems. The channel characteristics are never fixed and vary with movement of the mobile or its surroundings. So the channel is time-variant. These variations require complicated design problems to be solved for securing continued support during a single call, as the terminal moves through the service area. Radio design parameters are chosen to prevent the user as much as possible from experiencing corresponding fluctuations in service quality and reliability.

Apart from the atmospheric effects on the radio waves, the wave propagation may also be influenced by many obstacles such as buildings, hills and even other vehicles between the transmitter and the receiver. So propagation takes place in multipaths [7]. And that is why the instantaneous field strength at the mobile terminal is highly variable. For example radio signals exchanged between a base station and a mobile terminal in a typical urban environment exhibits extreme fluctuations in the amplitude as shown in Figure 2.1.

The prediction of the effect of propagation on system performance parameters is very useful in cellular system design [4,5]. It can provide information to insure uniform coverage and avoidance of co-channel interference. Moreover, the occurrence of handoff in the cellular system can be predicted more accurately.

2.2 SMALL-SCALE FADING AND MULTIPATH PROPAGATION

In the cellular radio environment, the mobile antennas are generally lower than some of the surrounding structures. Consequently, the waves transmitted from or to the base station are often effected by these structures. Reflected, refracted and scattered waves are generated. Summing all these waves at the receiver antenna results in a fast variation of the received signal. This is called *multipath fading*. The amplitude, phase and angle of arrival (*AOA*) of each of these waves are random variables. Assuming the phase and *AOA* are uniformly distributed, the short-term statistics of the resultant signal envelope fluctuations over local geographic areas approximate a Rayleigh probability density function (pdf). The Rayleigh fading of the mobile radio signals is generally uncorrelated.

The corresponding short-term power (average power measured over a number of RF cycles) of the desired signal, P_d , is exponentially distributed around the local mean power, P_{od} :

$$f_{P_d}(P_d | P_{od}) = \frac{1}{P_{od}} e^{-\frac{P_d}{P_{od}}} \quad (2.1)$$

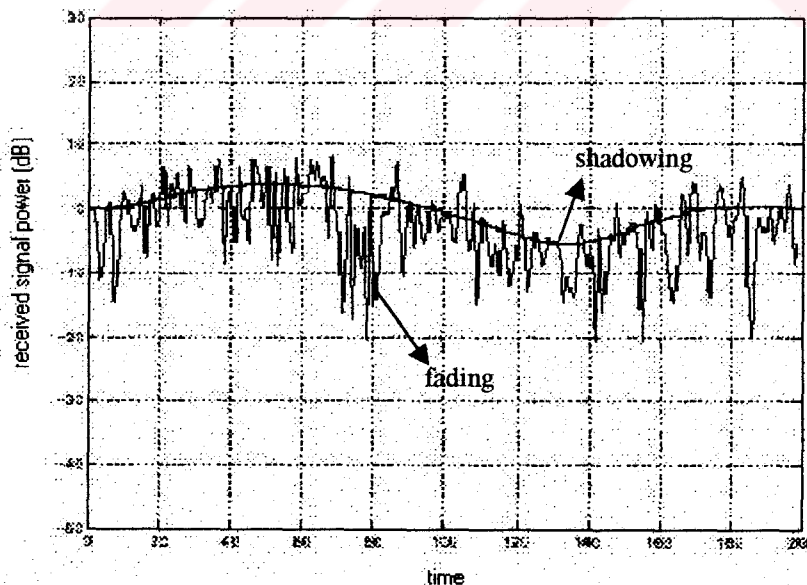


Figure 2.1 Typical variation of the received signal power with combined fading and shadowing

2.3 LARGE-SCALE FADING AND LOG-NORMAL SHADOWING

A mobile radio signal envelope is composed of two parts: a fast fading signal and a slow fading (shadowing) signal [8,9]. The local mean power of the signal can be obtained by smoothing out (averaging) the Rayleigh fading part, and retaining the slow fading part. Shadowing of the mobile radio signal by buildings or hills lead to slow changes in the local mean level, as the mobile terminal moves. The pdf of the local mean signal level is a log-normal distribution. Assuming that the desired and interfering signals are correlated, the joint pdf of the local mean powers of the desired, P_{od} , and the sum of interfering signals, P_{ou} , may be written as:

$$f_{P_{od}, P_{ou}}(P_{od}, P_{ou}) = \frac{e^{-\frac{\tau_d^2 + \tau_u^2 - 2\rho_{d,u}\tau_d\tau_u}{2(1-\rho_{d,u}^2)}}}{2\pi\sigma_d\sigma_u P_{od}P_{ou}\sqrt{1-\rho_{d,u}^2}} \quad (2.2)$$

$$\tau_d = \frac{1}{\sigma_d} \ln\left(\frac{P_{od}}{\xi_d}\right) \quad (2.3)$$

$$\tau_u = \frac{1}{\sigma_u} \ln\left(\frac{P_{ou}}{\xi_u}\right) \quad (2.4)$$

Here, σ_d , P_{od} and ξ_d are defined as, respectively, the standard deviation, the local mean power and the area mean power of the desired signal. Similarly, σ_u , P_{ou} and ξ_u stand for, respectively, the standard deviation, the local mean and the area mean power of the sum of interfering signals. The sum of the powers of a finite number of log-normally distributed signals can be approximated, at least as a first order, by another log-normal pdf. Note that $\rho_{d,u}$ is the correlation coefficient between the desired and the sum of interfering signals [10].

Since the propagation path changes as the mobile terminal moves, the path loss value of a received signal varies over different propagation paths. The path loss fluctuation and the terrain configuration profile at corresponding locations prove to be strongly correlated. Consequently, the local mean powers of the signals whose paths go through

the same terrain configurations are also correlated. The received signal is strong when the mobile terminal is at the top of a hill and weak when it is in a valley. The configuration of the terrain affects the standard deviation of the log-normal distribution representing the local mean signal in that area. The standard deviation of the local mean lies between 6-12 dB and with larger standard deviations generally found in more heavily built-up urban areas. Thus the standard deviation is a reflection of how much variation there is in the terrain contour.

Since the obstacles are mostly closer to the mobile terminals, shadowed signals are likely to be correlated in down-links (from base stations to mobile terminals) rather than in up-links (from mobile terminals to base stations). For realistic scenarios in cellular radio systems, the correlation coefficients between the individual signals may vary between 0.4 and 0.6. Nevertheless, these values depend on the angular separation between the directions of arrival and are expected to decrease with increasing angular separation.

In an environment with pure shadowing, the propagation medium is characterized by a joint log-normal pdf of the local mean powers of the desired and the sum of the interfering signals, which are in general correlated. When they are uncorrelated, the joint pdf can be written as the product of log-normal pdf's of the desired and the sum of interfering signals.

In a combined shadowing and fading environment, the short term power of the cumulative interference is exponentially distributed around the local mean power, which in turn, has a log-normal pdf around the area mean power. See Figure 2.2.

2.4 LARGE-SCALE PATH LOSS

Another important aspect of propagation between the base station and a mobile terminal is the prediction of the area mean signal level as a function of range. The area mean power, around which the local mean power is log-normally distributed, has a d^{-n}

type dependence. The distance: d between the base and the mobile has the path loss exponent n , which is between 2 and 4. To determine the received powers in terms of

$$P_r = \frac{P_t C}{d^a \left(1 + \frac{d}{g}\right)^b} \quad (2.5)$$

the path-loss and the transmitted power levels, we use a dual slope path-loss model, where the received signal power, P_r , and the transmitted power, P_t , are related by;

where C is a constant and d denotes the distance between the transmitter and the receiver. For $d \ll g$, the so-called turning point, the attenuation of the transmitted signal power with distance is given by d^{-a} ($a \approx 1.5, 2$) while, for $d \gg g$, the path-loss is described by $d^{-(a+b)}$ with $b \approx 2$. The path-loss is based on a two-path (direct and earth reflected) propagation model, for which the turning point is given by $g = 4h_t h_r / \lambda$ (h_t and h_r respectively denote the heights of the transmitting and receiving antennas and λ is the wavelength). Empirical data in the UHF band shows that g lies between 100m and 200m, depending on the antenna heights and the frequency of operation.

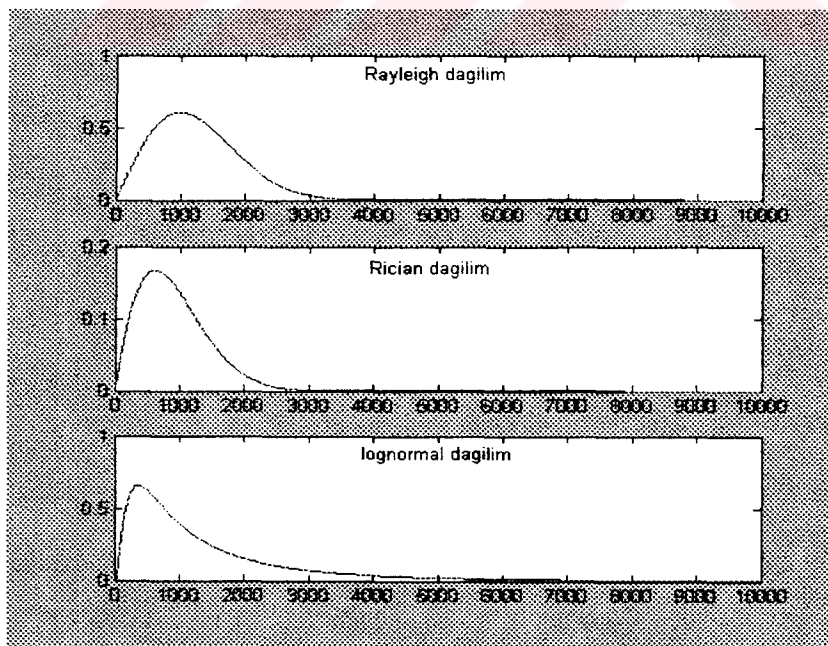


Figure 2.2 Rayleigh, Rice and log-normal pdf's

CHAPTER-3

PERFORMANCE IMPROVEMENT

3.1 THE MEASURE OF PERFORMANCE

The performance of a cellular radio system is usually measured in terms of the co-channel interference probability (PCI) and bit error rate (BER). BER gives a good indication of the performance of a particular modulation scheme. However, it does not provide information about the types of errors. For example it does not show incidents of bursty errors. In a fading mobile channel, it is likely that a transmitted signal will suffer deep fades, which can lead to the outage or complete loss of the signal. Probability of outage is another performance measure for a mobile communications system. It is the probability of failing to obtain satisfactory reception in the presence of interference. An outage event is specified by a specific number of bit errors occurring in a given transmission.

3.2 PROBABILITY OF CO-CHANNEL INTERFERENCE

The fundamental parameters in the design of cellular radio systems are: transmitter power, cell radius, normalized frequency reuse distance, cluster size and spectrum efficiency. In order to design any cellular system and determine system parameters, it is important to estimate the effect of PCI caused by a number of co-channel interferers [11,12].

The total PCI in cellular radio systems with hexagonal cellular layouts is contributed by a maximum of six co-channel interferers and is defined by:

$$F(CI) = \sum_{n=1}^6 \binom{6}{n} a_c^n (1 - a_c)^{6-n} F(CI | n) \quad (3.1)$$

where n denotes the number of active co-channel interferers and a_c stands for the carried traffic per channel in *erlang*. The conditional PCI, $F(CI|n)$, is given by:

$$F(CI | n) = \Pr(v < \alpha) = \int_0^\alpha \int_0^\infty f_{P_d, P_u}(vx, x) x dx dv \quad (3.2)$$

where α is the co-channel protection ratio and $v = P_d/P_u$ with P_d and P_u , respectively, denoting the short-term powers of the desired and the sum of n interfering signals.

In a *combined fading and shadowing environment*, the received signal consists of a fast fading signal superimposed on a shadowing signal. The joint pdf of the short-term powers of the desired and the sum of interfering signals may then be written as:

$$f_{P_d, P_u}(P_d, P_u) = \int_0^\infty \int_0^\infty f_{P_d}(P_d | P_{od}) f_{P_{od}, P_{ou}}(P_{od}, P_{ou}) f_{P_u}(P_u | P_{ou}) dP_{od} P_{ou} \quad (3.3)$$

the joint pdf of the local mean power levels of the desired and the sum of interfering signals, undergoing correlated log-normal shadowing, is given by:

$$f_{P_{od}, P_{ou}}(P_{od}, P_{ou}) = \frac{e^{-\frac{\tau_d^2 + \tau_u^2 - 2\rho_{d,u}\tau_d\tau_u}{2(1-\rho_{d,u}^2)}}}{2\pi\sigma_d\sigma_u P_{od} P_{ou} \sqrt{1-\rho_{d,u}^2}} \quad (3.4)$$

Here, $\tau_d = (1/\sigma_d) \ln(P_{od}/\xi_d)$ with ξ_d , σ_d and P_{od} being respectively the area mean power, the standard deviation and the local mean power of the desired signal. The corresponding parameters for the sum of interfering signals are denoted by τ_u , ξ_u , σ_u and P_{ou} . Note that $\rho_{d,u}$ denotes the correlation coefficient between the desired and the sum of n interfering signals. For $\rho_{d,u}=0$, (3.3) and (3.4) may be written as the product of two terms as functions of the pdf's of, respectively the desired and the sum of interfering signals.

The short-term power of the desired signal, P_d , undergoing Rician fading is:

$$f_{P_d}(P_d | P_{od}) = \frac{1}{P'_{od}} e^{-\frac{P_d + P_{sd}}{P'_{od}}} I_0 \left(\frac{2\sqrt{P_d P_{sd}}}{P'_{od}} \right) \quad (3.5)$$

where $I_0(x)$ is the modified Bessel function of the first kind and zero order. The local mean power of the desired signal, P_{od} is equal to the sum of the specular, P_{sd} and diffuse components, P'_{od} , i.e., $P_{od} = P_{sd} + P'_{od} = P'_{od}(1+K_d)$, with the Rice factor $K_d = P_{sd} / P'_{od}$. For $K_d = P_{sd} = 0$, (3.5) corresponds to Rayleigh faded desired signal.

The pdf of the *incoherent cumulation* of n Rician faded interfering signal powers is given by n -fold convolution of their pdf's. If these interfering signals have the same local mean power, then the pdf of the sum is given by:

$$f_{P_u}(P_u | P_{ou}) = \frac{e^{-\frac{P_u + P_{su}}{P'_{oi}}}}{P'_{oi}} \left(\frac{P_u}{P_{su}} \right)^{\frac{n-1}{2}} I_{n-1} \left(\frac{2\sqrt{P_u P_{su}}}{P'_{oi}} \right) \quad (3.6)$$

where $P'_{oi} = P_{oi} / (1+K_i)$ with P_{oi} and K_i being defined as, respectively, the local mean power and the Rice factor of an individual interferer and $P_{su} = n K_i P'_{oi} = K_i P_{ou} / (1+K_i)$. When the interfering signal powers are exponentially distributed ($P_{su} = K_i = 0$), using $I_x \approx [(x/2)^x / \Gamma(x+1)]$ for $x \rightarrow 0$, (3.6) can be shown to reduce to the convolution of the pdf's of n exponentially distributed interfering signals, i.e., gamma distribution. The *coherent cumulation* of n exponentially distributed random variables is also described by an exponential distribution with a mean equal to P_{ou} .

Using (3.2)-(3.6), lengthy manipulations lead to:

$$f(CI | n) = \frac{1}{\sqrt{2\pi}} \int_{-\infty}^{\infty} e^{-\frac{t^2}{2}} g(t) dt \quad (3.7)$$

where $g(t)$ is given by:

$$g(t) = 1 - \left(\frac{R}{1+R} \right)^n e^{\left(\frac{nK_i}{1+R} - K_d \right)} \sum_{k=0}^{\infty} \frac{K_d^k}{k!} \sum_{j=0}^k \frac{1}{(1+R)^j} \sum_{m=0}^j \binom{j+n-1}{j-m} \frac{1}{m!} \left(\frac{nK_i R}{1+R} \right)^m \quad (3.8)$$

and R is given by:

$$R = \frac{n (K_i + 1) \left(\frac{G + R_u}{G + 1} \right)^b}{\alpha (K_d + 1)} R_u^a e^{(m_d - m_u + \sigma_e t)} \quad (3.9)$$

with $\sigma_e^2 = \sigma_d^2 + \sigma_v^2 - 2\rho_{d,u} \sigma_d \sigma_u$. R_u and G denote, respectively, the frequency reuse distance and the turning point of the path loss curve, both normalized with respect to the cell radius. The standard deviation, σ_u , the logarithmic mean power, m_u of the sum of n correlated log-normal interfering signals as well as the correlation coefficient, $\rho_{d,u}$, was determined by the method presented.

When the interfering signals undergo Rayleigh fading ($K_i=0$), taking only $m=0$ term in the last summation in leads to:

$$g(t) = 1 - \frac{R^n e^{-K_d}}{(1+R)^n} \sum_{k=0}^{\infty} \frac{K_d^k}{k!} \sum_{j=0}^k \binom{j+n-1}{j} \frac{1}{(1+R)^j} \quad (3.10)$$

For *coherent cumulation* of n Rayleigh-faded interferers, the expression corresponding to (3.10) is:

$$g(t) = \frac{n}{n+R} e^{\frac{-K_d R}{n+R}} \quad (3.11)$$

For Rayleigh-faded desired and interfering signals; $K_d=K_i=0$, $g(t)$ in (3.10) reduces to:

$$g(t) = 1 - \left(\frac{R}{1+R} \right)^n \quad (3.12)$$

In case of *pure shadowing*, the conditional PCI is found by directly inserting (3.4) into (3.2) with $P_d=P_{od}$ and $P_u=P'_{ou}$;

$$F(CI | n) = \frac{1}{\sqrt{2\pi}} \int_{p/\sigma_e}^{\infty} e^{-\frac{t^2}{2}} dt \quad (3.13)$$

$$p = m_d - m_u - \ln \alpha + \ln \left[R_u^a \left(\frac{G + R_u}{G + 1} \right)^b \right] \quad (3.14)$$

3.3 PROBABILITY OF A BIT ERROR

The BER in cellular radio systems is given by [11,12]:

$$P_e = \sum_{n=1}^6 \binom{6}{n} P_n(e|n) a_c^n (1 - a_c)^{6-n} \quad (3.15)$$

where n denotes the number of active co-channel interferers and a_c stands for the carried traffic per channel in erlang. The BER, $P_n(e|n)$, conditioned on the presence of n active co-channel interferers in a pure Rician fading environment for non-coherent DPSK and FSK, is given by:

$$P_n(e|n) = \frac{1}{2(1+R)} e^{\left(\frac{-K_d R}{1+R}\right)} \quad (3.16)$$

where R is defined by:

$$R = \frac{P_{0d} T_b}{A P_{0u} T_b + B N_0} = \frac{1}{1 + K_d} \left[\frac{1}{\frac{A}{P_{0d}/P_{0u}} + \frac{B}{E_b/N_0}} \right] \quad (3.17)$$

For non-coherent DPSK; $A=B=1$, for non-coherent FSK; $A=B=2$. Here, E_b / N_0 denotes the ratio of the local-mean energy per bit of the desired signal to noise density.

$$\frac{E_b}{N_0} = \frac{P_{0d} T_b}{N_0} \quad (3.18)$$

Assuming that the desired signal and n individual co-channel interferers have the same transmitted power, the ratio of the received local-mean power levels of the desired signal and cumulative co-channel interference is found as;

$$\frac{P_{0d}}{P_{0u}} = \frac{1}{n} R_u^a \left(\frac{G + R_u}{G + 1} \right)^b \quad (3.19)$$

where $R_u = D / R$ and $G = g / R$ denote, respectively, the frequency reuse distance and the turning point, both normalized with respect to the cell radius.

The conditional BER, for Rician faded desired signal with shadowed LOS component, may be written as:

$$P_n(e|n) = \frac{1}{2\sqrt{2\pi}(1+R)} \int_{-\infty}^{\infty} e^{-\frac{t^2}{2}} e^{\frac{-K_d'R}{1+R} e^{\sigma_{sd}t}} dt \quad (3.20)$$

where

$$K_d' = \frac{e^{m_{sd}}}{P_{od}'} \quad (3.21)$$

The conditional BER for signals undergoing correlated shadowing may be written as:

$$P_n(e|n) = \int_{-\infty}^{\infty} \int_{-\infty}^{\infty} \frac{1}{2(1+R)} e^{\left(\frac{K_d'R}{1+R}\right)} f_{P_{od}, P_{ou}}(P_{od}, P_{ou}) dP_{od} dP_{ou} \quad (3.22)$$

A variable transformation between P_{od} and τ_d and between P_{ou} and τ_u followed by another transformation with $x=\tau_d$ and $y=(\tau_u-\rho_{d,u}\tau_d)/(1-\rho_{d,u}^2)^{1/2}$ leads to the following expression for the conditional BER:

$$P_e(e|n) = \frac{1}{4\pi} \int_{-\infty}^{\infty} \int_{-\infty}^{\infty} e^{-(x^2+y^2)} \frac{e^{\frac{K_d'R}{1+R}}}{1+R} dx dy \quad (3.23)$$

Here, R is still given by (3.17) with the exception that, P_{od} and P_{ou} are now random with area mean powers ξ_d and ξ_u . The shadowed version of E_b / N_0 may be written as:

$$\frac{E_b}{N_0} = \frac{T_b \xi_d}{N_0} e^{\sigma_d x} \quad (3.24)$$

Similarly, the shadowed version of P_{od} / P_{ou} is given by:

$$\frac{P_{od}}{P_{ou}} = \left(\frac{G+R_u}{G+1} \right)^b R_u^a e^{\left(m_d - m_u + (\sigma_d - \sigma_u \rho_{d,u})x - \sigma_u \sqrt{1 - \rho_{d,u}^2} y \right)} \quad (3.25)$$

Here, $m_d = \ln(\xi_d)$ and σ_d denote, respectively, the logarithmic mean and the shadow spread of the desired signal while $m_u = \ln(\xi_u)$ and σ_u are the corresponding parameters for the sum of n correlated co-channel interferers. Here,

$$x = \tau_d = \ln(P_{od} / \xi_d) / \sigma_d \quad (3.26)$$

$$y = (\tau_u - \rho_{d,u} \tau_u) / (1 - \rho_{d,u}^2)^{1/2} \quad (3.27)$$

$$\tau_u = \ln(P_{od} / \xi_u) / \sigma_u \quad (3.28)$$

CHAPTER-4

IMPROVING COVERAGE AND CAPACITY IN CELLULAR SYSTEMS

As the demand for wireless service increases, the number of channels assigned to a cell eventually becomes insufficient to support the required number of users. At this point, cellular design techniques are needed to provide more channels per unit coverage area. Techniques such as *cell splitting*, *sectorization*, and *coverage zone approaches* are used in practice to expand the capacity of cellular systems [13].

4.1 CELL SPLITTING

Cell splitting is the process of subdividing a congested cell into smaller cells, each with its own base station and a corresponding reduction in antenna height and transmitter power. See Figure 4.1.

Cell splitting increases the capacity of a cellular system, since it increases the number of times that channels are reused. By defining new cells which have a smaller radius than the original cells and by installing these smaller cells (called microcells) between the existing cells, capacity increases due to the additional number of channels per unit area [1].

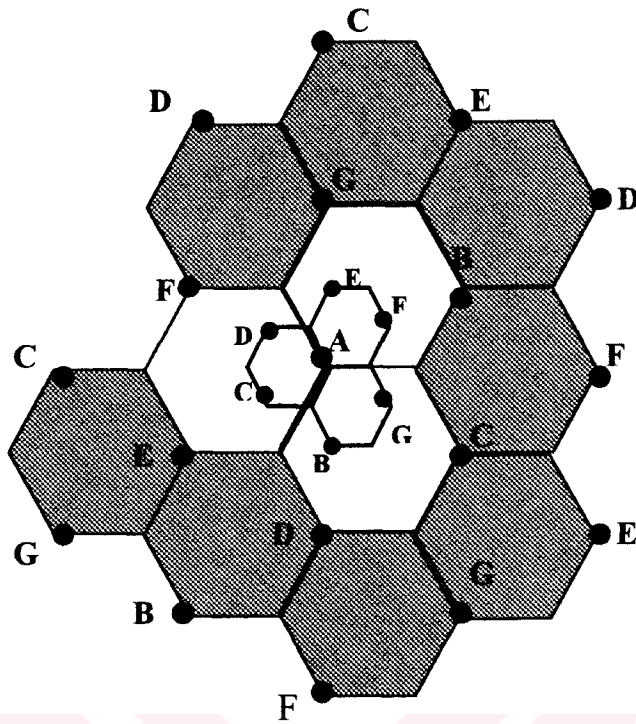


Figure 4.1 Cell Splitting

For the new cells to be smaller in size, the transmit power of these cells must be reduced. The transmit power of the new cells with radius half that of the original cells can be found by examining the received power P_r at the new and old cell boundaries and setting them equal to each other. This is necessary to ensure that the frequency reuse plan for the new microcells behaves exactly as for the original cells. For Figure 4.1

$$P_r \text{ [at old cell boundary]} \propto P_{t1} \cdot R^{-n} \qquad P_r \text{ [at new cell boundary]} \propto P_{t2} \cdot (R/2)^{-n}$$

where P_{t1} and P_{t2} are the transmit powers of the larger and smaller cell base stations, respectively, and n is the path loss exponent. If we take $n=4$ and set the received powers equal to each other, then;

$$P_{t2} = \frac{P_{t1}}{16} \qquad (4.1)$$

4.2 SECTORIZATION

The co-channel interference in a cellular system may decrease by replacing a single omnidirectional antenna at the base station by several directional antennas, each radiating within a specified sector. By using directional antennas, a given cell will receive interference and transmit with only a fraction of the available co-channel cells. This technique for decreasing co-channel interference and thus increasing system performance by using directional antennas is called *sectorization*. The factor by which the co-channel interference is reduced depends on the amount of sectoring used [14]. A cell is normally partitioned into three 120° sectors or six 60° sectors as shown in Figure 4.2.

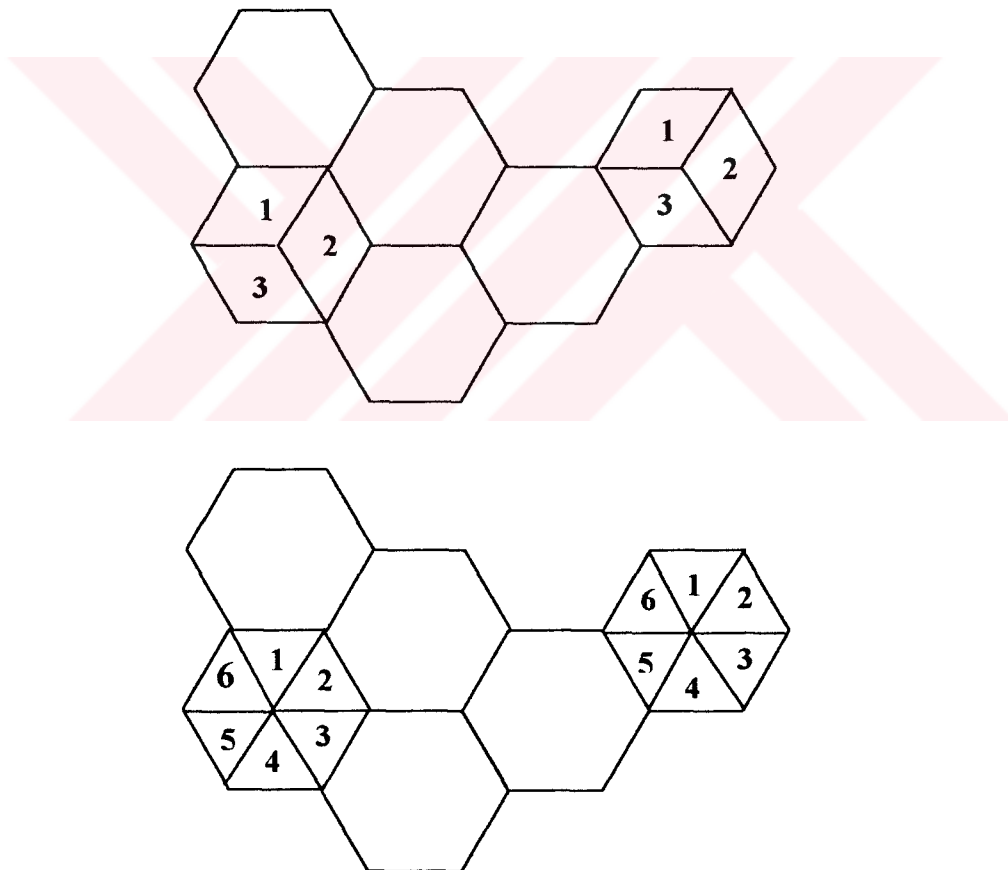


Figure 4.2 Sectors in 120° and 60° sectorization

4.2.1 Design of an Omnidirectional Antenna System

In the start-up phase of a system, omnidirectional antennas are used mainly because of their lower initial cost. In a fully equipped hexagonal shaped cellular system, there are always six co-channel interfering cells in the first tier, as shown in Figure 4.3. The six co-channel interfering cells in the second tier cause weaker interference than those in the first tier. Therefore the co-channel interference from the second tier of interfering cells is negligible.

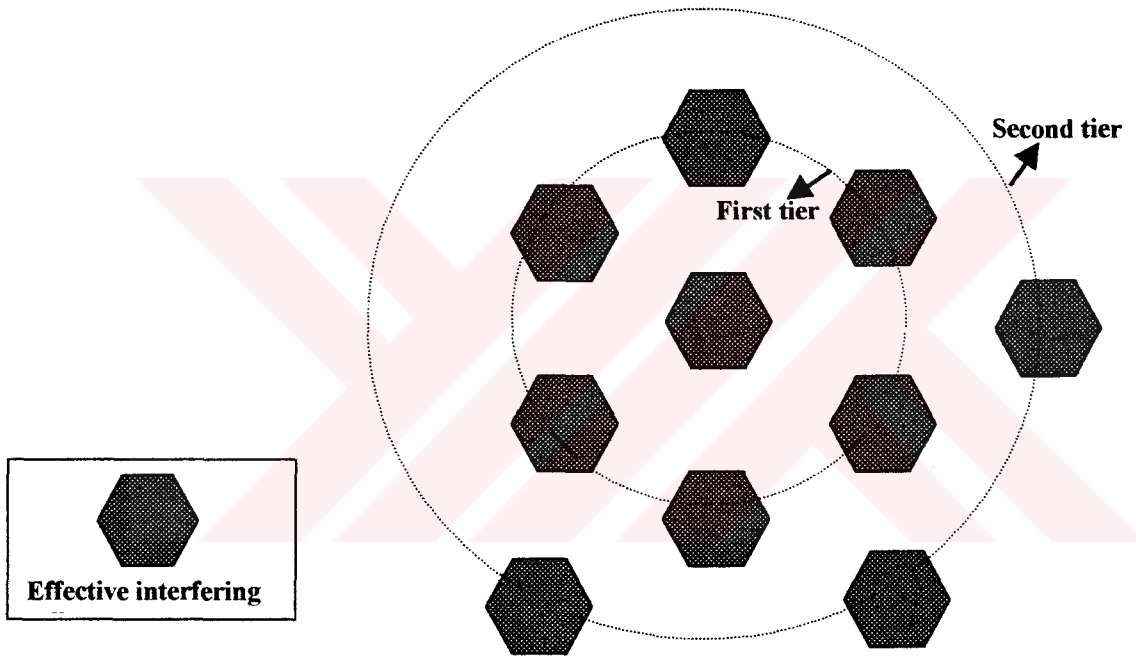


Figure 4.3 First and second tiers in the cellular system

In the worst case the mobile unit is at the cell boundary R , as shown in Figure 4.4. The distances from all six co-channel interfering sites are also shown. The carrier-to-interference power ratio is:

$$\frac{\xi_d}{\xi_u} = \frac{R^{-4}}{2(D-R)^{-4} + 2D^{-4} + 2(D+R)^{-4}} = \frac{1}{2(R_u - 1)^{-4} + 2R_u^{-4} + 2(R_u + 1)^{-4}} \quad (4.2)$$

To be conservative, we may use the shortest distance D-R for all six interferers as a worst case, then ξ_d / ξ_u ratio is replaced by:

$$\frac{\xi_d}{\xi_u} = \frac{R^{-4}}{6(D-R)^{-4}} = \frac{1}{6(R_u - 1)^{-4}} \quad (4.3)$$

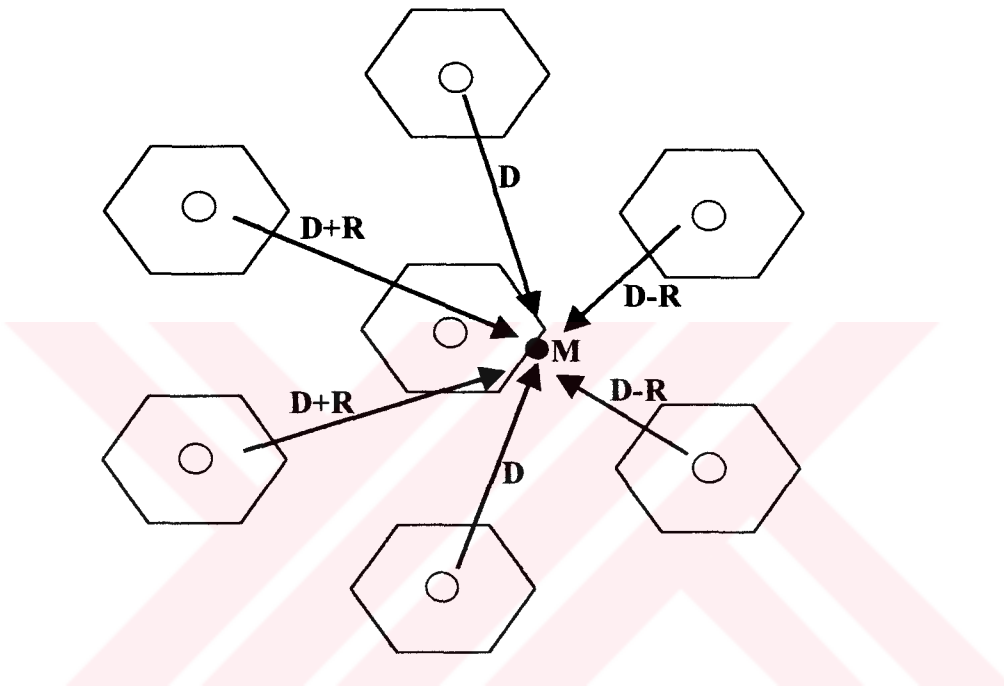


Figure 4.4 Co-channel interference, worst case in omnidirectional antenna system

4.2.2 Design of a Directional Antenna System

In addition to using guard band between the channels and using geographical separation between co-channel cells to reduce interference, the directional antennas could be used to further eliminate the interference. When the traffic begins to increase, the frequency spectrum needs to be used more efficiently and avoid increasing the number of cells per cluster. The co-channel interference may be reduced by using directional antennas which can direct signals into their service area and substantially reduce the interference to the co-channel cells outside their main lobe. Using

directional antennas, the PCI can be reduced by more than half since the strong co-channel interference comes from the back cells but not from the front cells. Therefore, directional antenna system can potentially operate with a smaller frequency reuse distance. In these systems, each cell is divided into three or six sectors, thus three or six directional antennas are used at each base station as shown in Figure 4.5.

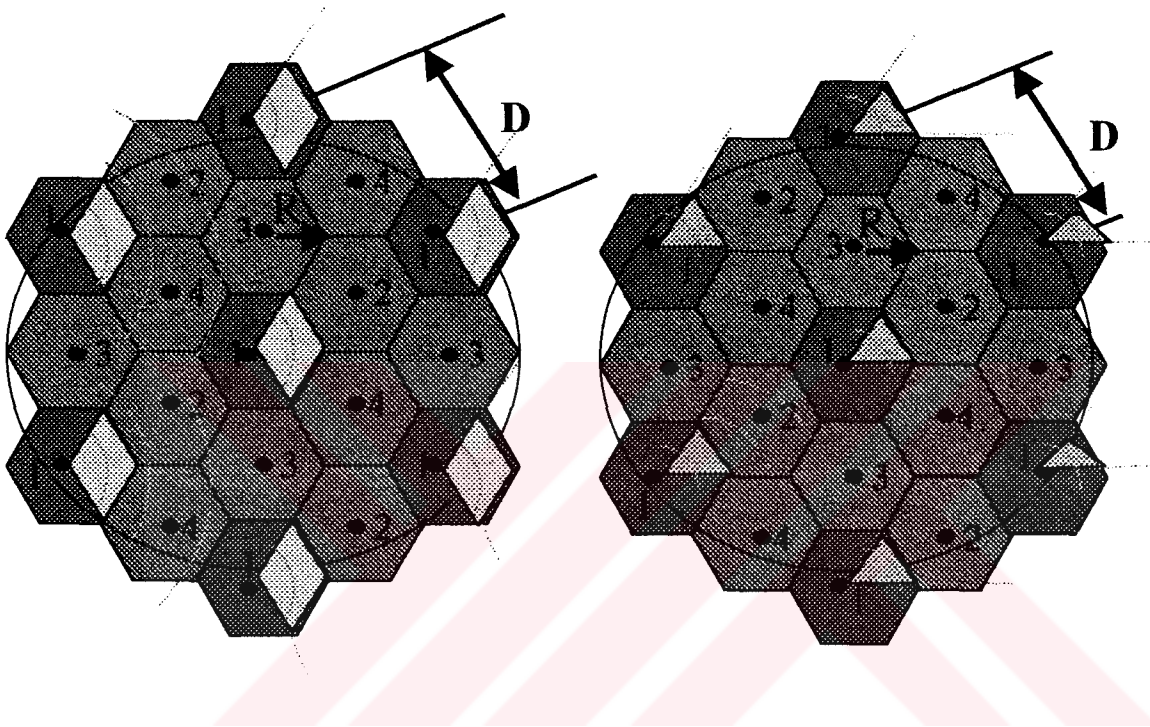


Figure 4.5 a) interferers in 120° and b) 60° sectoring

4.2.2.1 Directional Antennas in C=7 Cell Patterns

a) Three-sector case

The three-sector case is shown in Figure 4.6. The mobile unit will experience greater interference in the lower shaded cell-sector than in the upper shaded cell-sector. This is because the mobile unit receives the weakest signal from its own cell, but fairly strong interference signal from the interfering cells. In a three-sector case, the interference is effective in only one direction because the front-to-back ratio of a cell-site directional

antenna is at least 10 dB or more in a mobile radio environment. Because of the using directional antennas, the number of principal interferers is reduced from six to two. The worst case of ξ_d / ξ_u occurs when the mobile is at position M, at which point the distance between the mobile unit and the two interfering antennas is roughly $D + R/2$. The value ξ_d / ξ_u can be obtained by the following expression:

$$\frac{\xi_d}{\xi_u} = \frac{R^{-4}}{(D+0.7R)^{-4} + D^{-4}} = \frac{1}{(R_u + 0.7)^{-4} + R_u^{-4}} \quad (4.4)$$

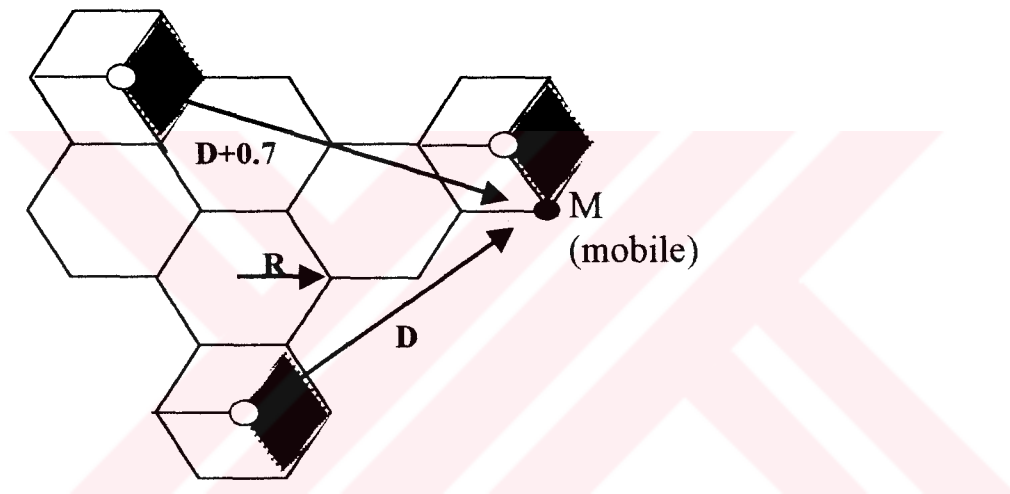


Figure 4.6 Co-channel interference, worst case in 120° sectoring

b) Six-sector case

We may also divide a cell into six sectors by using six 60°-beam directional antennas as shown in Figure 4.7. In this case, only one instance of interference can occur in each sector. Therefore, the carrier-to-interference ratio in this case is;

$$\frac{\xi_d}{\xi_u} = \frac{R^{-4}}{(D+0.7R)^{-4}} = (R_u + 0.7)^4 \quad (4.5)$$

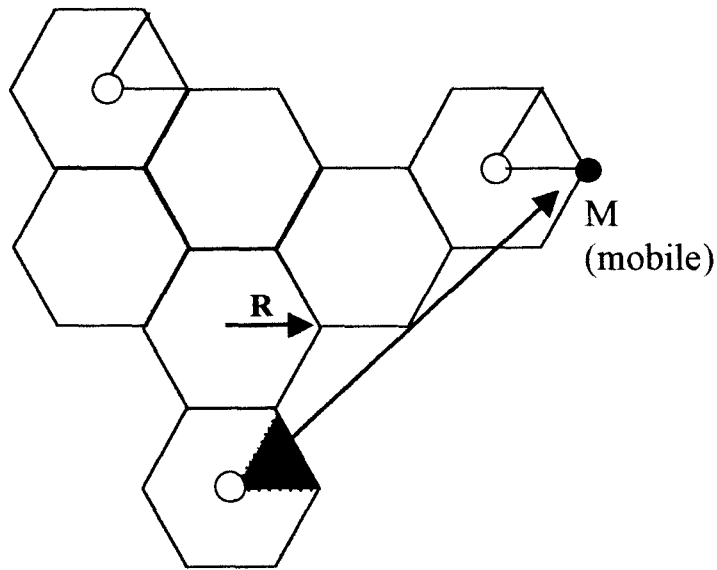


Figure 4.7 Co-channel interference, worst case in 60° sectoring

4.2.2.2 Directional Antennas in C=4 Cell Patterns

a) Three-sector case

To obtain the carrier-to-interference ratio, we use the same procedure as in the C=7 cell pattern system. The 120°-beam directional antennas used in the sectors reduced the interferers to two as in C=7 and $R_u = \sqrt{3C} = 4.6$ systems. For C=4, the value of $R_u = \sqrt{3C} = 3.46$.

$$\frac{\xi_d}{\xi_u} = \frac{1}{(R_u + 0.7)^{-4} + R_u^{-4}} = 20\text{dB} \quad (4.6)$$

b) Six-sector case

There is only one interferer at a distance of D+R with $R_u = 3.46$, we can obtain

$$\frac{\xi_d}{\xi_u} = \frac{R^{-4}}{(D+R)^{-4}} = \frac{1}{(R_u + 1)^{-4}} = 27\text{dB} \quad (4.7)$$

4.3 RESULTS AND CONCLUSIONS

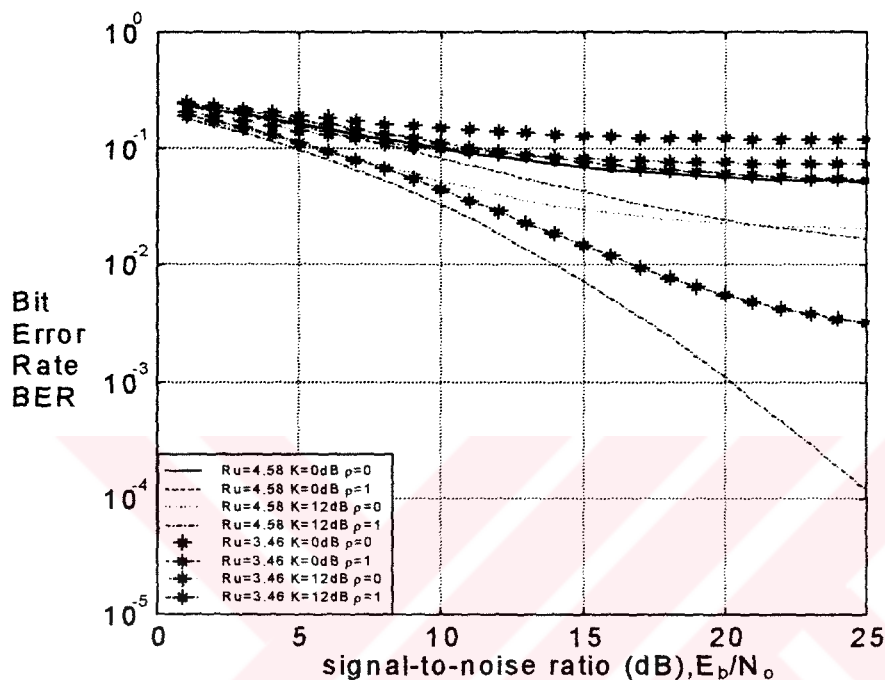


Figure 4.8 Effect of R_u , K_d , ρ and E_b/N_0 on BER for omnidirectional antenna systems under shadowing and Rician/Rayleigh fading.

Figure 4.8 shows the effects of normalized frequency reuse distance (R_u), Rice factor (K_d), correlation coefficient between the signals (ρ), and the ratio of the energy per bit to the noise spectral density (E_b/N_0) on Bit Error Rate (BER) for omnidirectional antenna systems. Here, the signals are assumed to be Rician distributed. Note that K_d plays a more dominant role in determining the BER in a correlated shadowing environment compared to the uncorrelated case ($\rho=0$) and this role becomes more significant at larger values of E_b/N_0 . BER can be reduced by using larger frequency reuse distance.

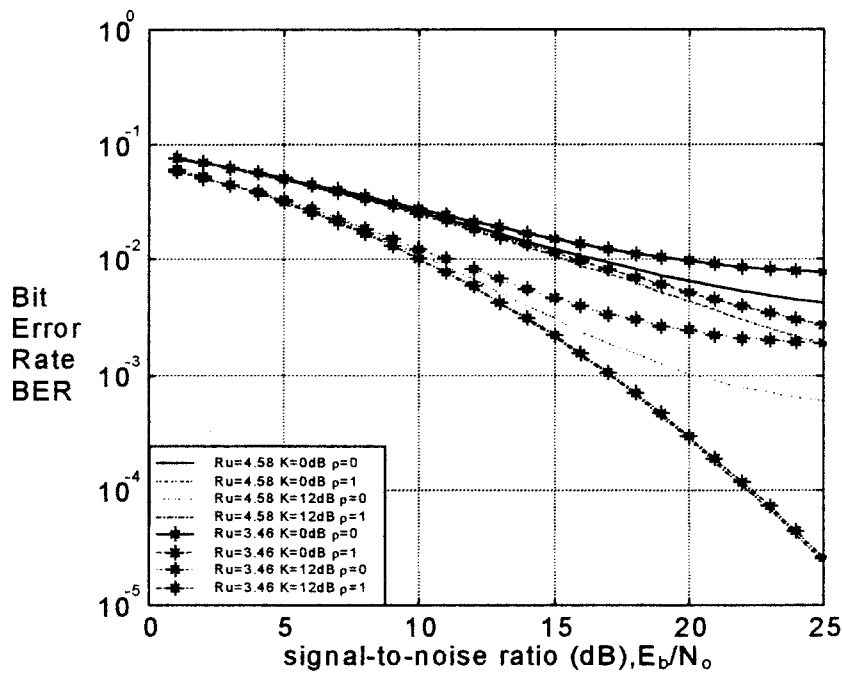


Figure 4.9 Effect of R_u , K_d , ρ and E_b/N_0 on BER for 120° directional antenna systems under shadowing and Rician/Rayleigh fading.

Figure 4.9 shows the effects of normalized frequency reuse distance (R_u), Rice factor (K_d), correlation coefficient between the signals (ρ), and the ratio of the energy per bit to the noise spectral density (E_b/N_0) on BER for 120° directional antenna systems. Note that, using 120° directional antennas leads to improved BER performance compared to the omnidirectional antenna systems (Figure 4.8).

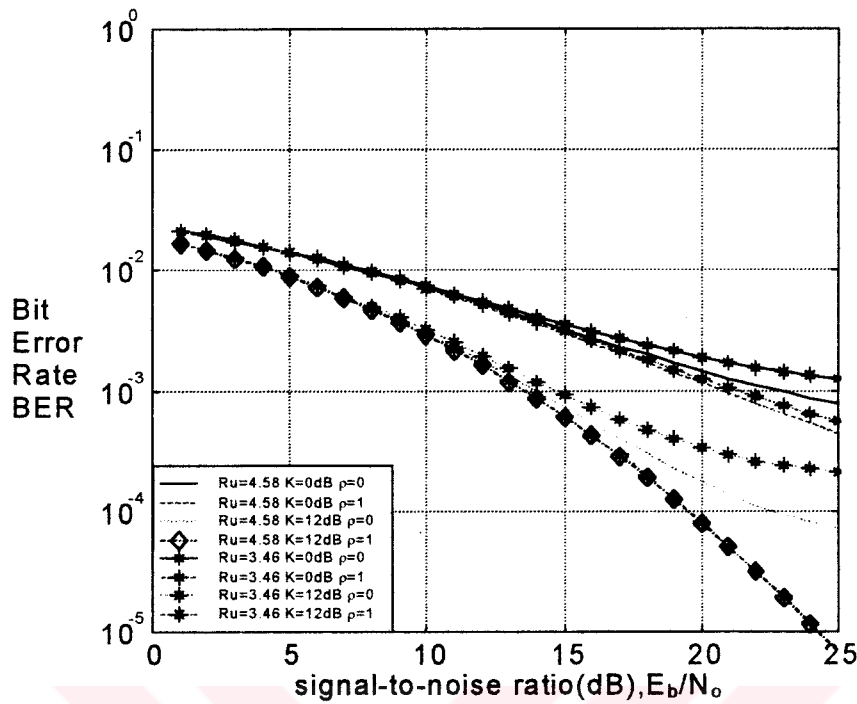


Figure 4.10 Effect of R_u , K_d , ρ and E_b/N_0 on BER for 60° directional antenna systems under shadowing and Rician/Rayleigh fading.

Figure 4.10 shows the effects of normalized frequency reuse distance (R_u), Rice factor (K_d), correlation coefficient between the signals (ρ), and the ratio of the energy per bit to the noise spectral density (E_b/N_0) on BER for 60° directional antenna systems. We can also divide a cell into six sectors by using six 60° -beam directional antennas as shown in Figure 4.5b. In this case, only one instance of interference can occur in each sector. Therefore, we can get further reduction in BER level compared to the omnidirectional and 120° directional antenna systems.

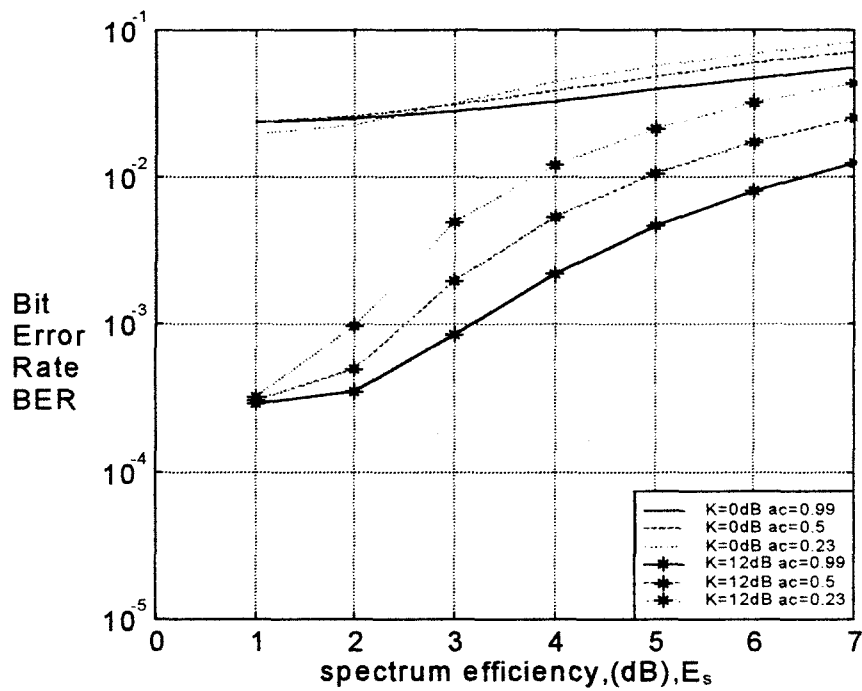


Figure 4.11 Effect of K_d and traffic per channel (a_c) on spectral efficiency for *omnidirectional* antenna systems under shadowing and Rician/Rayleigh fading.

Figure 4.11 shows the effects of Rice factor (K_d) and traffic per channel (a_c) on the spectral efficiency for omnidirectional antenna systems under shadowing and Rician/Rayleigh fading. For a fixed BER, increased values of the Rice factor and traffic per channel lead to higher spectral efficiencies.

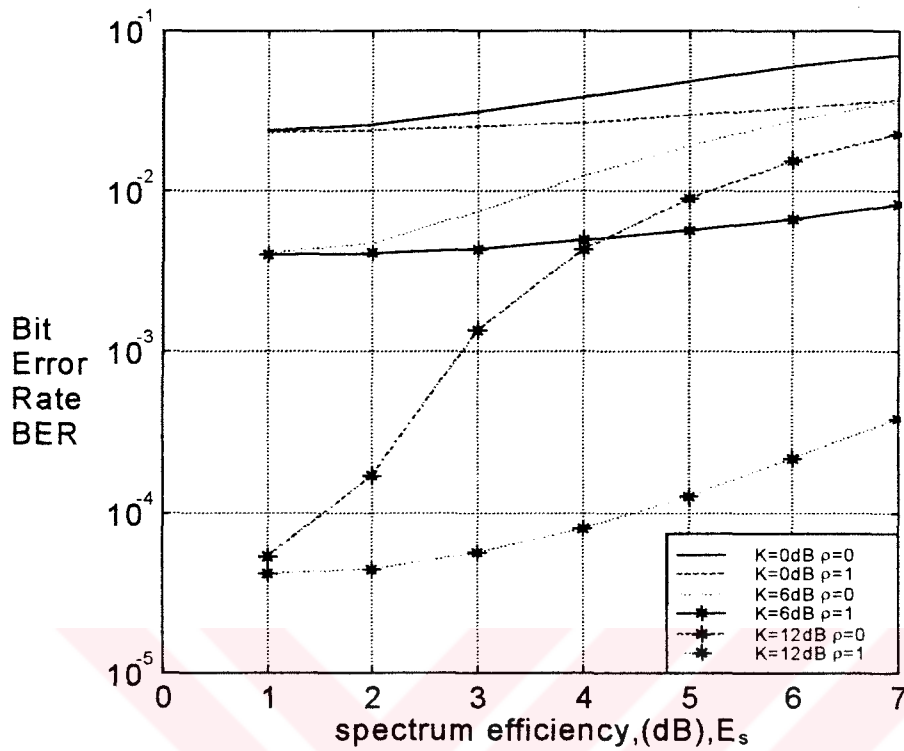


Figure 4.12 Effect of K_d and correlation coefficient (ρ) on the spectrum efficiency for *omnidirectional* antenna systems under shadowing and Rician/Rayleigh fading.

Figure 4.12 shows the effects of Rice factor (K_d) and correlation coefficient between the signals (ρ) on the spectrum efficiency for omnidirectional antenna systems. For a fixed BER, increased values of the Rice factor and correlation coefficient between the signals lead to higher spectral efficiencies.

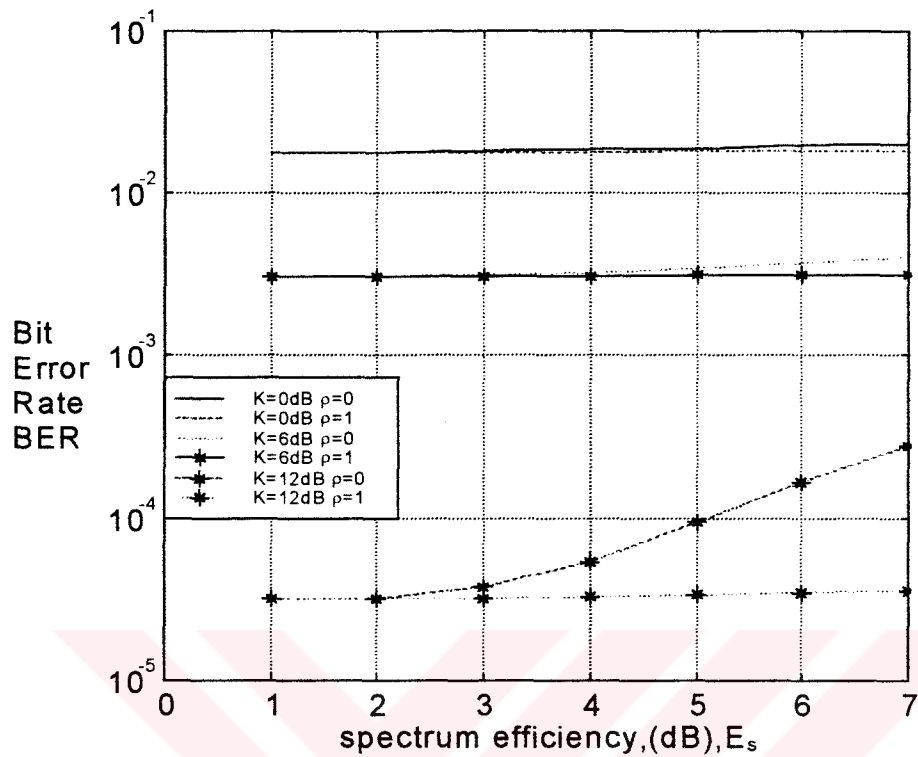


Figure 4.13 Effect of K_d and correlation coefficient (ρ) on the spectrum efficiency for 120° directional antenna systems under shadowing and Rician/Rayleigh fading.

Figure 4.13 shows the effects of Rice factor (K_d) and correlation coefficient between the signals (ρ) on the spectrum efficiency for 120° directional antenna systems. BER level can be reduced by using directional antennas as shown in Figure 4.13.

BER level can be reduced by using directional antennas. This means that each cell is divided into three or six sectors and uses three or six directional antennas at a base station. Each sector is assigned a set of frequencies (channels). Because of the use of directional antennas, the number of principal interferers is reduced from six to two (120° sectors) or one (60° sectors). Therefore, using directional antenna systems can improve system performance and increase the system capacity.

CHAPTER 5

SMART ANTENNAS

Smart antennas are basically an extension of beam sectorization in which the sector coverage is supplanted by multiple beams. This is achieved by the use of array structures, and the number of beams in the sector is a function of the array extent.

The increase in beam directionality can provide an increase in capacity and expand cell site geographic coverage. The former is more applicable to urbanized areas and the latter to rural areas. At the mobile end (uplink mode), the benefit accrued by reducing transmitter power, because of the greater gain of the base station antenna, can extend the life of the battery.

The increased rejection of interference by the use of multiple beams: (1) permits a tighter reuse structure; (2) can improve the quality of voice communications through the vehicle by an increase in ξ_d / ξ_u (>18 dB); and (3) can reduce multipath, thus tempering the power margin requirements. Smart antenna systems can include both switched beam and adaptive antenna technologies as shown in Figure 5.1a and 5.1b.

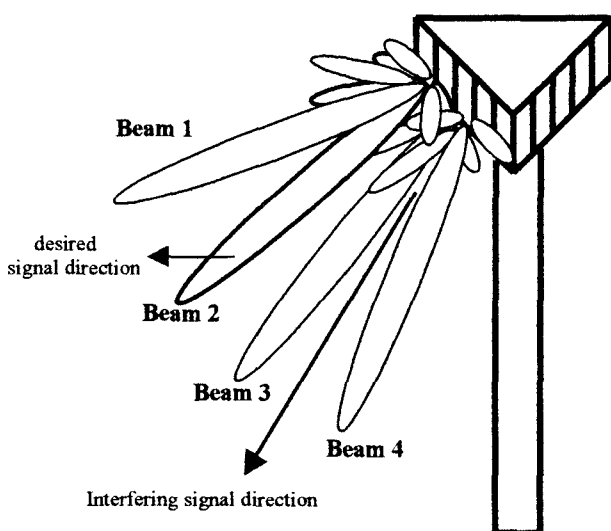


Figure 5.1a Switched-beam system

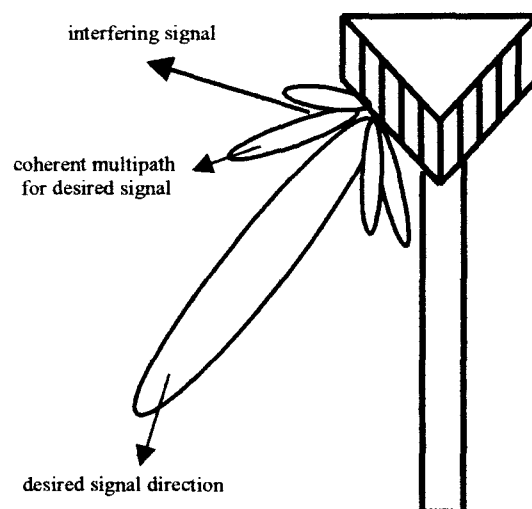


Figure 5.1b Adaptive antenna

5.1 SWITCHED-BEAM SYSTEMS

Switched-beam systems use a number of fixed beams at an antenna site. The receiver selects the beam that provides the greatest signal enhancement and interference reduction. The output to the beams is either RF or baseband digitally processed to ascertain the sector in which the communicating mobile may be located. The cellular space is broken down into three sectors (120°), with each sector served by an array of radiating elements fed by a beamforming network, which ideally forms independent beams. A typical display of these beams at a cell site is shown in Figure 5.2. The figure shows five beams in each 120° sector, with a nominal beamwidth of 24° in azimuth. Switched-beam systems may not offer the degree of performance improvement offered by the adaptive systems, but they are often much less complex and are easier to retro-fit to existing wireless technologies.

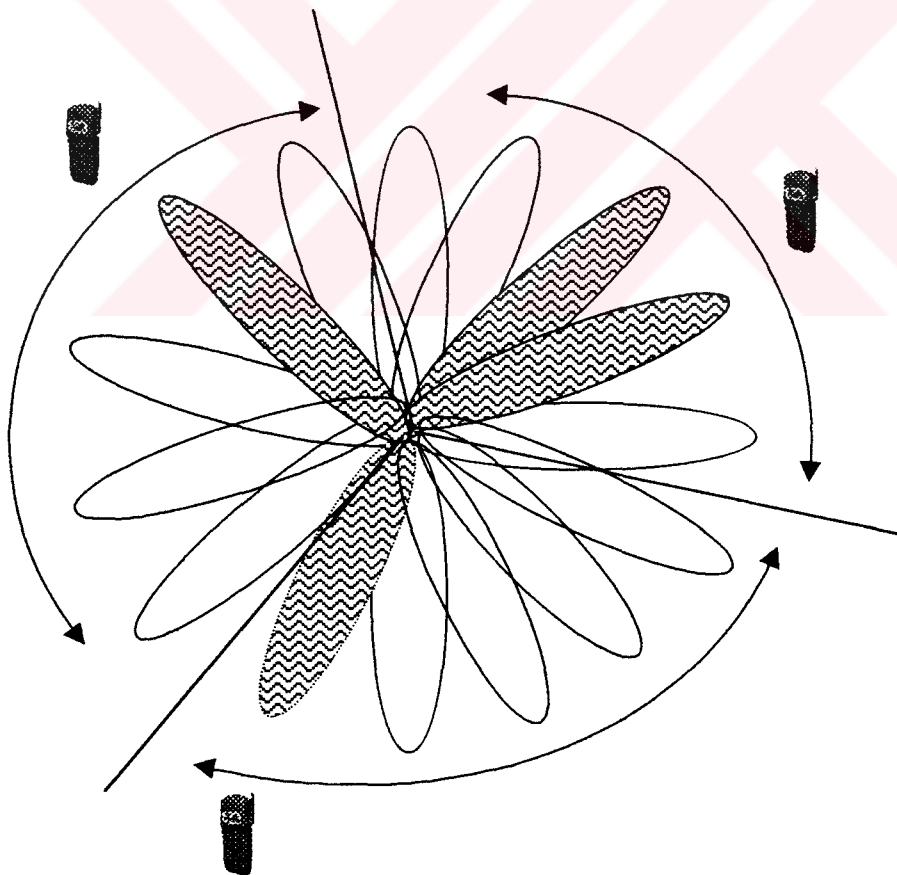


Figure 5.2 A rosette of directional beams for a smart antenna.

5.2 ADAPTIVE ANTENNA SYSTEMS

In a phased array receiving antenna, the signals received by the array elements are generally added at RF to form a receiving beam. In an adaptive array, both phase and amplitude of each element output are controlled by an adaptive network, that is, they use algorithms that iteratively adjust the weighting of the signals at the array elements. The signals are combined to maximize the signal-to-interference-plus-noise ratio: SINR and to eliminate interfering signals in any direction other than the main beam [15,16]. A simple form of this array is shown in Figure 5.3.

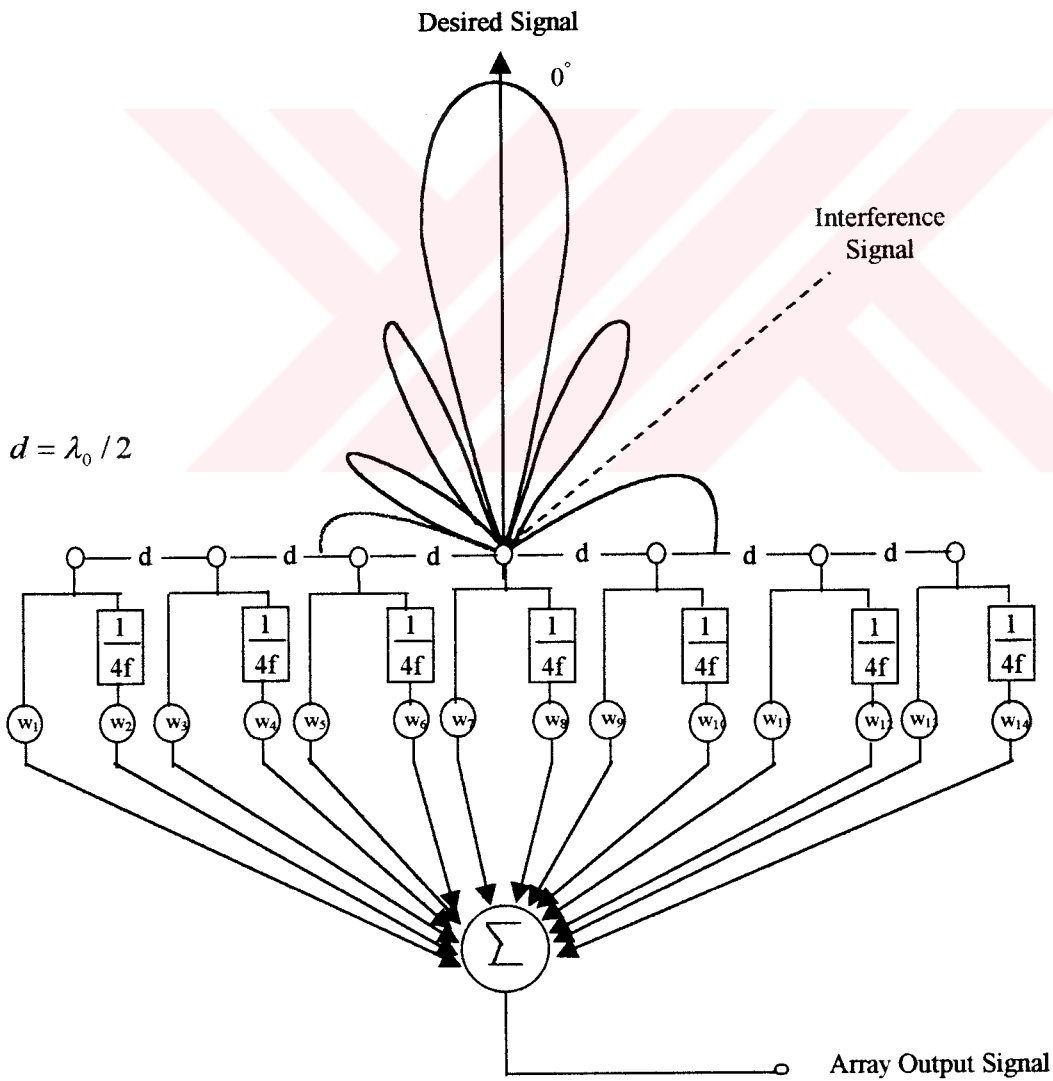


Figure 5.3 Uniformly spaced (d), 7-element linear adaptive array

The weights are controlled depending on the signal and the noise/interference level, as well as by the system requirements. These weights are complex and provide both amplitude and phase information. Output elements are: $x_1(t)$, $x_2(t)$, $x_3(t)$, ... , $x_N(t)$. The beam (assumed receiving) is formed by multiplying each $x_n(t)$ by a complex weight, w_n , and then summing the resultant signals. Both w_n and x_n are complex quantities in that they are variable in phase and amplitude.

By suitable choice of complex conjugate phase shifts in the weights, a beam can be steered to the direction of the desired angle, which gives a coherent summation of the individual inputs and a null in an interfering direction, that is, at an angle other than the desired direction. In cellular applications, when used at the base stations, they are capable of providing automatic adjustment of the far-field pattern to form nulls in the direction of interfering sources while maintaining high gain in the direction of the desired user.

5.3 RESULTS AND CONCLUSIONS

Adaptive antenna systems can trace the desired signal, while at the same time nulling the interferers. That is the property which makes them a hot research topic. In the following simulation study, a uniformly spaced 10-element linear adaptive array is under observation. The signals coming to the array are under flat Rayleigh fading. We have equal-power (same SIR) interferers coming from different but known directions. By changing the number of interferers the adaptive array's interference suppressing capability and error performance are analyzed. Adaptive antenna array uses the LMS (Least Mean Square) algorithm for adaptation. [17,18]

Figure 5.4a shows the radiation pattern of a 10-element, uniformly spaced linear adaptive array. There are two interfering signals coming to the array from -30° and 0° directions. The array is successful at placing its main beam to the desired signal direction which is 30° and nulls to the directions of interference for canceling them. In Figure 5.4b shown is the squared error of the adaptation process. The mean value is 3.273×10^{-5} .

Figure 5.5a shows the radiation pattern of the same array with 4 interferers coming in -60° , -45° , -30° and 0° directions. The deep nulls at these directions can be seen in the figure, as well as the main beam in the wanted signal direction. The plot of the squared error of the adaptation process is in Figure 5.5b. The mean value is 8.478×10^{-6} .

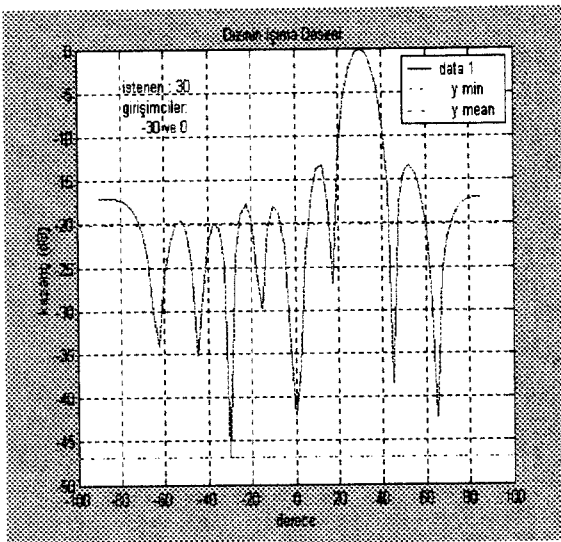


Figure 5.4a Radiation pattern of the uniformly spaced 10-element linear adaptive antenna array with 2 interferers coming from -30 and 0 degrees

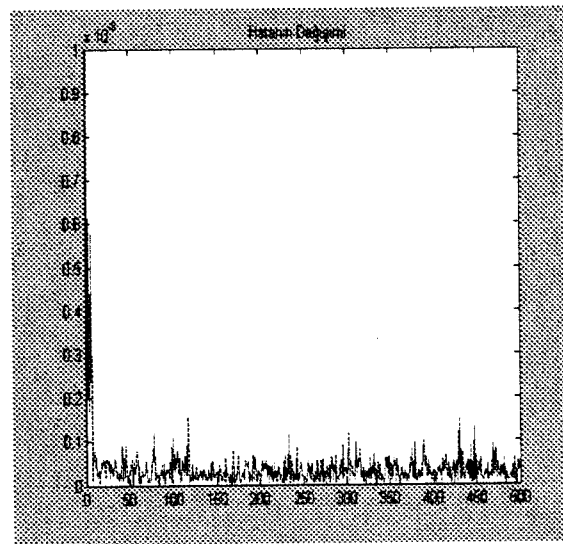


Figure 5.4b Squared error of the uniformly spaced 10-element linear adaptive array for the 2-interferer case

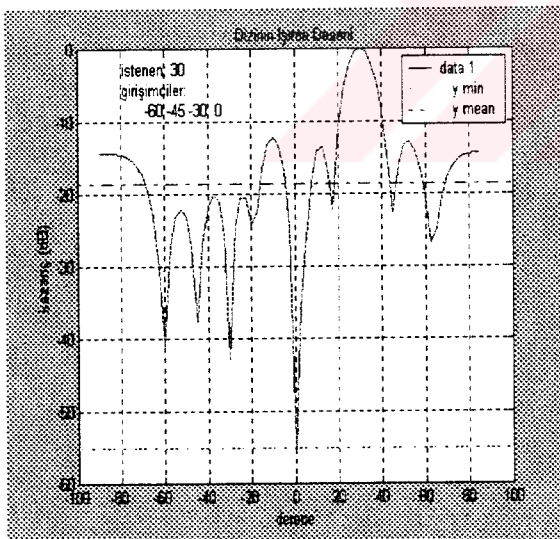


Figure 5.5a Radiation pattern of the uniformly spaced 10-element linear adaptive antenna array with 4 interferers coming from -60, -45, -30 and 0 degrees

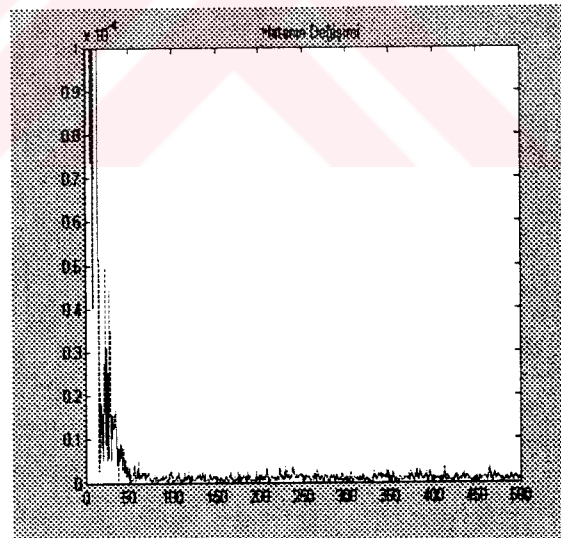


Figure 5.5b Squared error of the uniformly spaced 10-element linear adaptive array for the 4-interferer case

Shown in Figure 5.6a is the radiation pattern of the uniformly spaced, 10-element linear adaptive array for the case of 6 interference signals coming from -60° , -45° , -30° , -10° , 0° and 15° directions. The array is successful again in placing the nulls. In Figure 5.6b, the mean value of the squared error is 1.973×10^{-6} .

Finally in Figure 5.7a and 5.7b, seen in the figures are the radiation pattern of the uniformly spaced, 10-element linear adaptive array with 8 interferers coming from -60° , -45° , -30° , -10° , 0° , 15° , 45° and 75° directions and change of the squared error value, respectively. The mean value of the squared error is: 2.768×10^{-6} .

An adaptive array of M antenna elements can suppress up to $M-1$ interferers; and the results constitute four successful examples for this.

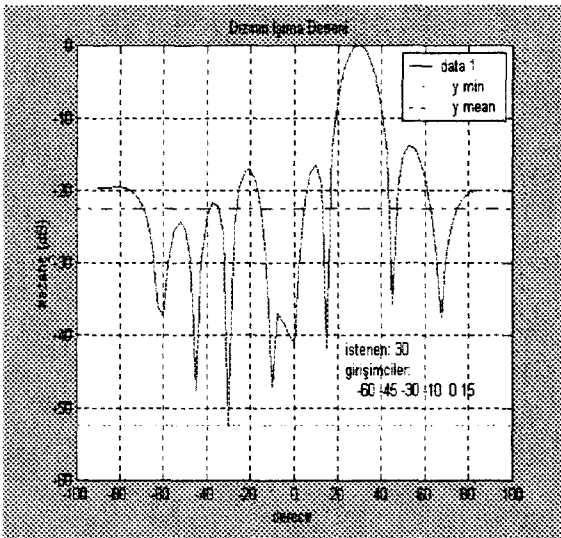


Figure 5.6a Radiation pattern of the uniformly spaced 10-element linear adaptive antenna array with 6 interferers coming from -60 , -45 , -30 , -10 , 0 and 15 degrees

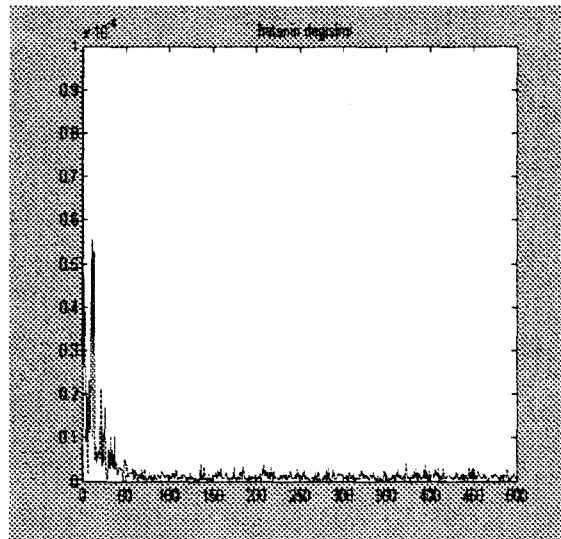


Figure 5.6b Squared error of the uniformly spaced 10-element linear adaptive array for the 6-interferer case

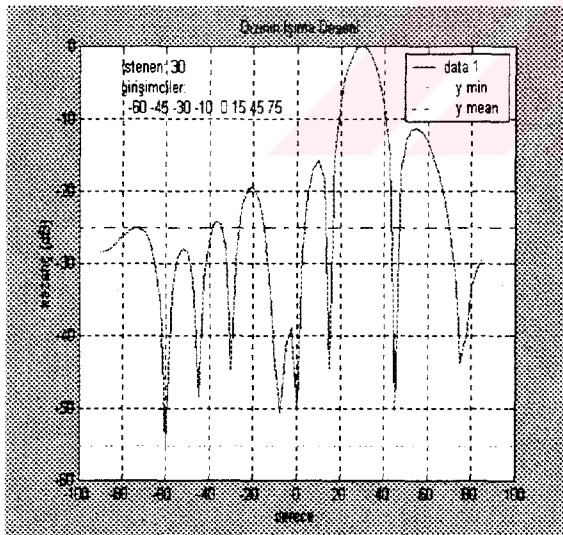


Figure 5.7a Radiation pattern of the uniformly spaced 10-element linear adaptive antenna array with 8 interferers coming from -60 , -45 , -30 , -10 , 0 , 15 , 45 and 75 degrees

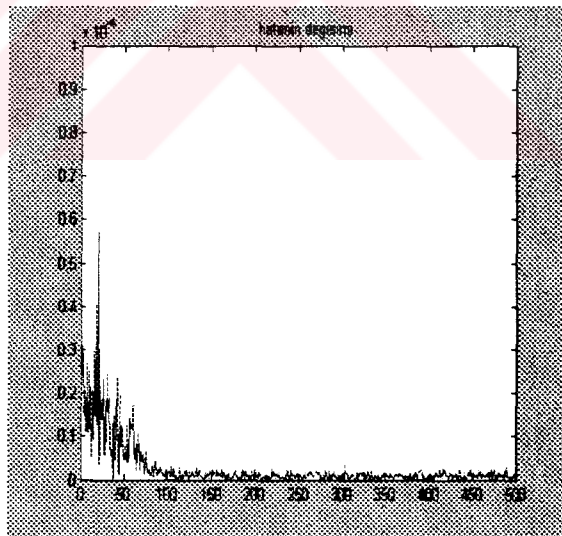


Figure 5.7b Squared error of the uniformly spaced 10-element linear adaptive array for the 8-interferer case

CHAPTER 6

ADAPTIVE BEAMFORMING IN MOBILE COMMUNICATIONS

Adaptive array systems have undergone enormous growth and progress in the past two decades. A primary reason for this growth is their ability to automatically respond to an unknown interference environment, in real-time, by steering nulls and reducing side lobe levels in the directions of the interference, while retaining some desired signal beam characteristics. These systems usually consist of an array of antenna elements (or beam parts) and a real-time adaptive receiver-processor which adjusts the element weights toward some optimization of output signal-to-noise ratio (SNR) in accordance with selected control algorithms. They adapt to the total signal environment “seen” by the array of sensors, using all available degrees-of-freedom (DOF) of the systems in an optimal sense. This contrasts sharply with a conventional antenna wherein the DOF are deterministically set and do not adapt to a changing input signal environment.

6.1 Operation of Adaptive Antenna Arrays

The adaptive array consists of a number of antenna elements, not necessarily identical, coupled together via some form of amplitude control and phase shifting network to form a single output. The amplitude and phase control can be regarded as a set of complex weights, as shown in Figure 6.1. If the effects of the receiver noise and mutual coupling are ignored, linear array can be explained as follows. Consider a wave front generated by a narrow-band source of wavelength λ arriving at a M element array from a direction θ_i off the array foresight. Now taking the first element in the array as the phase reference and letting “d” equal the array spacing, the relative phase shift of the received signal at the m^{th} element can be expressed as:

$$\phi_{mi} = \frac{2\pi d (m-1)}{\lambda} \sin(\theta_i) \quad (6.1)$$

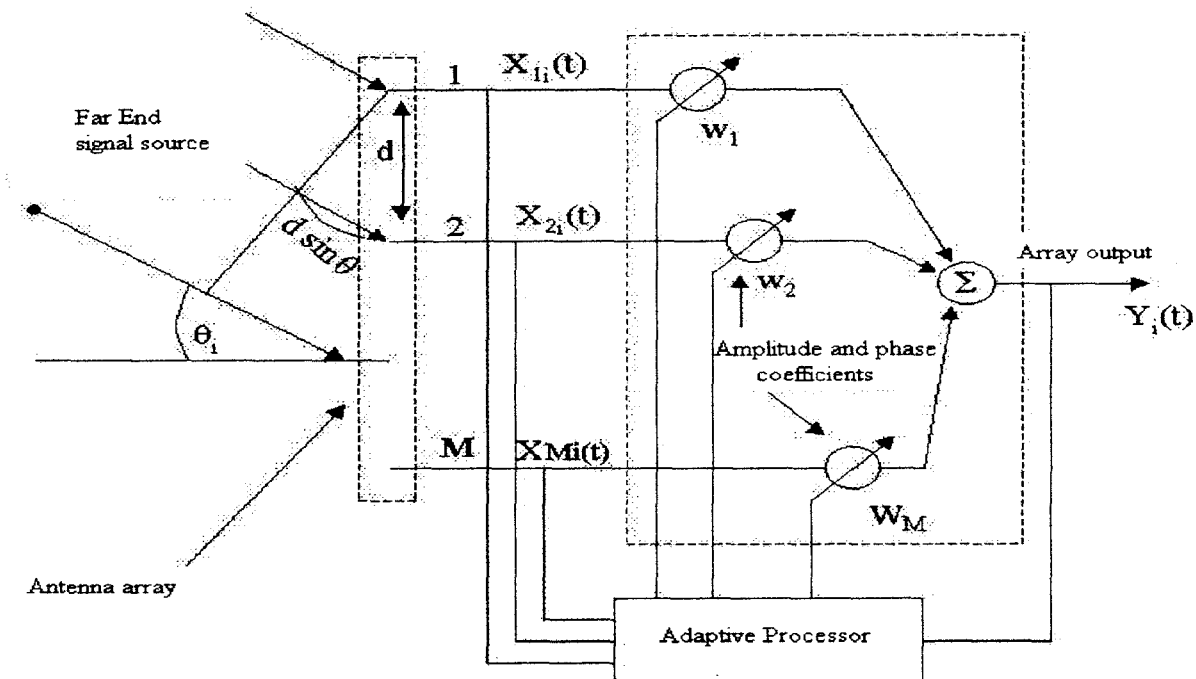


Figure 6.1 Adaptive antenna array

Assuming constant envelope modulation of the source at θ_i , the signal at the output of each of the antenna elements can be expressed as:

$$x_{mi}(t) = e^{j(\omega t + \phi_{mi})} \quad (6.2)$$

and the total array output in direction θ_i as:

$$y_i(t) = \sum_{m=1}^M w_m e^{j(\omega t + \phi_{mi})} \quad (6.3)$$

where w_m represents the value of the complex weight applied to the output of the m^{th} element. Thus by suitable choice of weights, the array will accept a wanted signal from direction θ_s and steer nulls toward interference sources located at θ_i , for $i \neq 1$.

The antenna elements can be arranged in various geometry's, with uniform line, circular and planar array being very common. In the circular array geometry, beams can be steered through 360°, thus giving complete coverage from a central base station. The elements are typically sited $\lambda/2$ apart, where λ is the wavelength of the received signal. Spacing of greater than $\lambda/2$ improves the spatial resolution of the array, however, the formation of grating lobes (secondary maxima) can also result. These are generally regarded as undesirable.

6.2 Reduction of Co-Channel Interference Using Adaptive Antennas

The use of adaptive antennas can reduce co-channel interference. The blocking probability B is the fraction of attempted calls that can not be allocated a channel. If there are A Erlangs of traffic intensity, the actual traffic carried is equal to $A(1-B)$ Erlangs. The outgoing channel usage efficiency can be defined as:

$$\eta = \frac{A(1-B)}{M} \quad (6.4)$$

where M is the total number of channels available per cell. In the case of adaptive antennas, there are μ beams in a cell and $M\mu / \mu$ channels per beam.

Since it is assumed that at any time all μ beams per cell are formed, there will always be six beams aligned onto the wanted mobile. Hence, for the adaptive antenna:

Probability that the interfering co-channel is in the beam pointing at the wanted mobile is the same as:

$$\text{(number of active channels in beam) / (total number of channels)}$$

and that is;

$$= \frac{A(1-B)/M}{M} = \frac{\eta}{\mu} \quad (6.5)$$

Let M_I be the number of active interfering co-channel cells. In practice, M_I is a random variable and has a pdf: $\text{Prob}(M_I)$ given by

$$\text{Prob}(M_I) = \binom{6}{M_I} \left(\frac{\eta}{\mu}\right)^{M_I} \left(1 - \frac{\eta}{\mu}\right)^{6-M_I} \quad (6.6)$$

which is also called the origination probability. The total co-channel interference probability can be written as:

$$\sum_M \text{Prob}\left(\frac{P_d}{P_u} \leq \alpha, \mu\right) = \sum_M \text{Prob}\left(\frac{P_d}{P_u} \leq \alpha / M\right) \binom{6}{M_I} \left(\frac{\eta}{\mu}\right)^{M_I} \left(1 - \frac{\eta}{\mu}\right)^{6-M_I} \quad (6.7)$$

6.3 RESULTS AND CONCLUSIONS

The following figures are the results of the study, which examined adaptive antenna systems analytically. The effects of signal (channel) correlation, standard deviation of shadowing (σ), modulation method and number of antenna elements, on the PCI are investigated for 1-interferer and 6-interferer cases [19]. In the figures, μ is the number of antenna elements in the array. See the graphics next page.



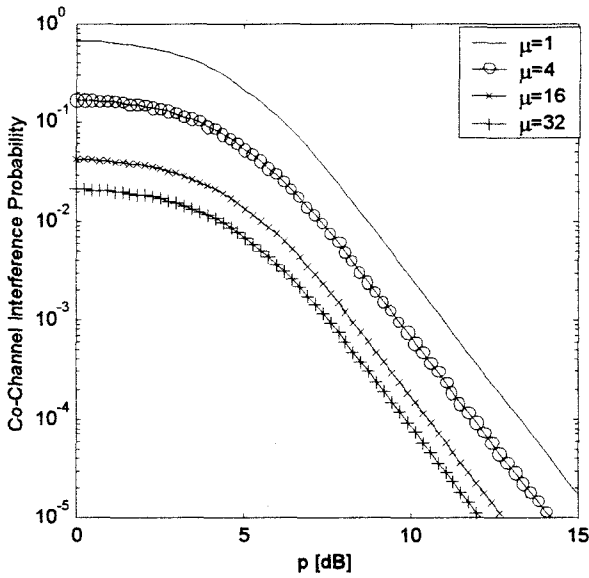


Figure 6.2 Effect of the number of antenna elements (μ) on the co-channel interference probability with: 1-interferer, $\sigma = 4\text{dB}$, $K_d = 6\text{dB}$, $\rho = 0$

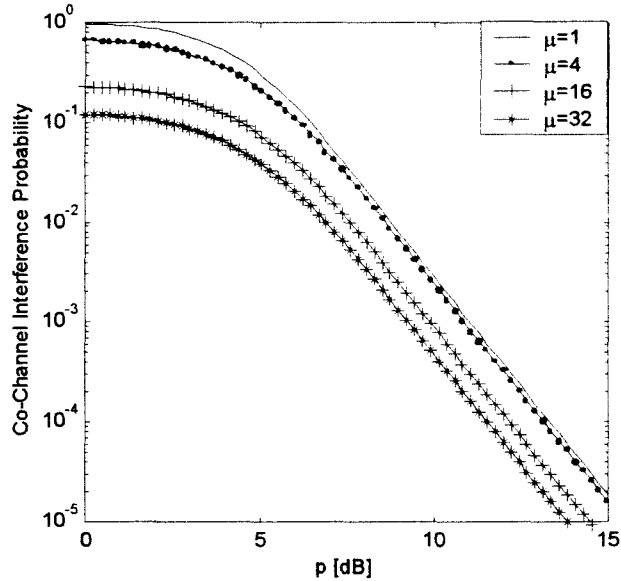


Figure 6.3 Effect of the number of antenna elements (μ) on the co-channel interference probability with: 6-interferer, $\sigma = 4\text{dB}$, $K_d = 6\text{dB}$, $\rho = 0$

Shown in Figure 6.2 is the effect of μ (number of antenna elements) on PCI for $\sigma = 4\text{dB}$, $K_d = 6\text{dB}$, $\rho = 0$. There is no correlation between the signal and the interferer, but both of them are under shadowing. Coherent interference probability is investigated for $\mu = 1, 4, 16, 32$. As seen; increasing the number of antenna elements in the array will decrease the probability of co-channel interference.

In Figure 6.3, the same scenery is valid; but this time there are 6 interferers. As expected, PCI is bigger than the previous case where there is only one interferer. Notice the decrease in the graphic for $\mu = 16$. We can say again; increasing μ , will decrease the probability of co-channel interference.

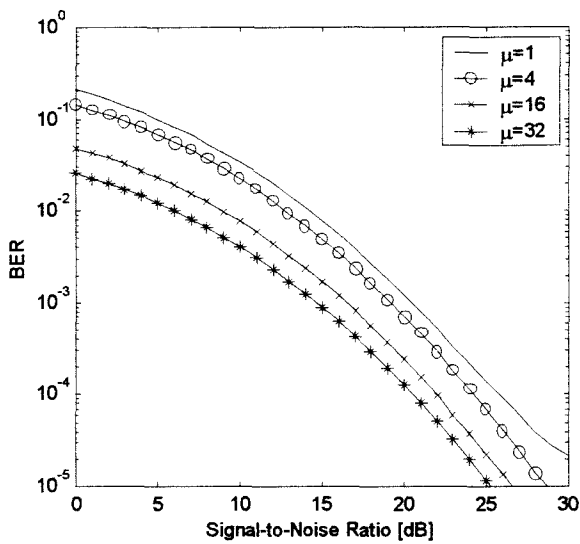


Figure 6.4 Effect of the number of antenna elements (μ) on BER with NCDPSK modulation.

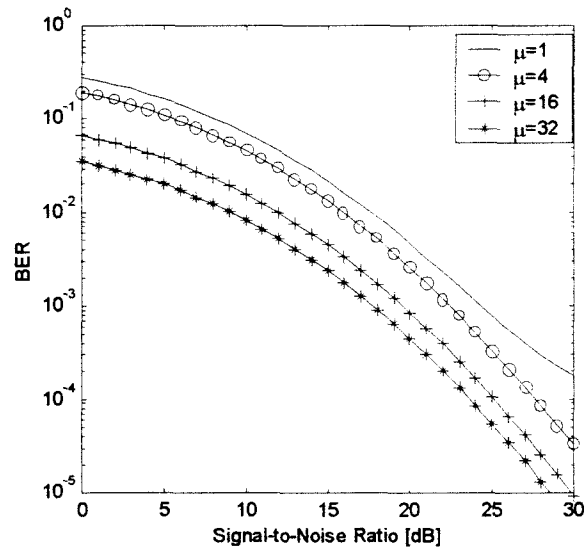


Figure 6.5 Effect of the number of antenna elements (μ) on BER with NCFSK modulation.

In Figure 6.4, shown is the change of the Bit Error Rate (BER) with four values of μ with NCDPSK modulation used in the system. In Figure 6.5, the same analysis is performed for NCFSK modulation. As the number of antenna elements increases bit error rate will decrease. We can also say that NCDPSK is more successful than NCFSK as seen in the graphics.

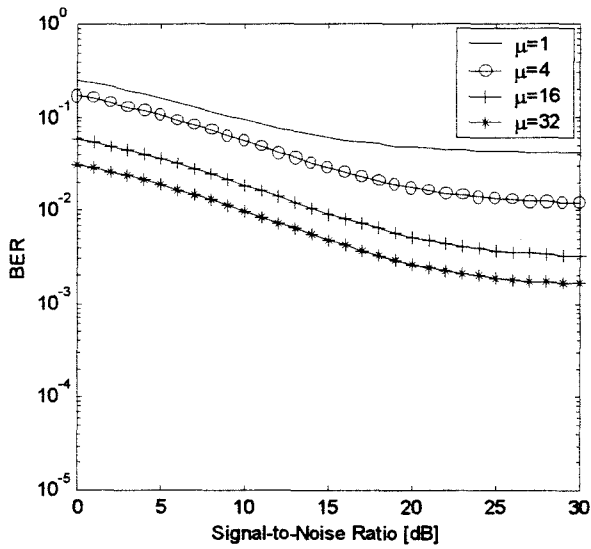


Figure 6.6 Effect of the number of antenna elements (μ) on BER with uncorrelated interferers ($\rho=0$)

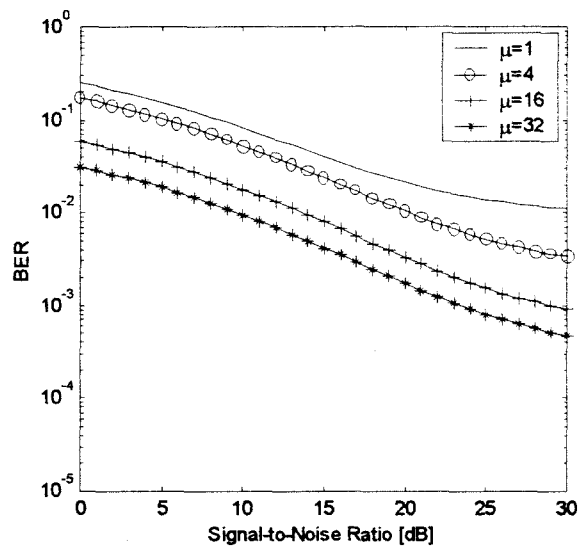


Figure 6.7 Effect of the number of antenna elements (μ) on BER with correlated interferers ($\rho=1$)

In Figure 6.6 and 6.7, we investigate the effect of the number of antenna elements on the bit error rate for correlated and uncorrelated interferers. As seen in the graphs, the adaptive array performs better with correlated interferers than with uncorrelated interferers.

CHAPTER-7

RESULTS AND CONCLUSIONS

In this study we investigated the spectrum efficiency gain and the improvement of performance using adaptive antenna arrays in cellular mobile communications systems. In the adaptive antenna systems, the signals received by the antennas are weighted and combined in such a way that the signal-to-interference plus noise ratio (SNIR) of the output is maximized, thereby reducing both the effects of Rayleigh fading of the desired signal and the co-channel interference. The use of adaptive antennas improves the performance of mobile communication systems in terms of probability of co-channel interference (PCI) and bit error rate (BER).

A comparison of omnidirectional, directional and adaptive antennas was performed in Chapter-4. BER level can be reduced by using directional antennas in a cell, which is called sectorization. This means that each cell is divided into generally three or six sectors and uses three or six directional antennas at a base station. Each sector is assigned a set of frequencies (channels). Because of the use of directional antennas, the number of principal interferers is reduced from six to two (120° sectors) or one (60° sectors).

We analyzed the effects of normalized frequency reuse distance (R_u), Rice factor (K_d), correlation coefficient between the signals (ρ), and the ratio of the energy per bit to the noise power spectral density (E_b/N_0) on BER for omnidirectional, 120° directional and 60° directional antenna systems (Figure 4.8, 4.9 and 4.10 respectively). Here, the signals are assumed to be Rician distributed. Rician factor (K_d) plays a more dominant role in determining the BER in a correlated shadowing environment compared to the uncorrelated case ($\rho=0$) and this role becomes more significant at larger values of E_b/N_0 . We also observe that BER can be reduced by using larger frequency reuse distance (R_u). To conclude, directional antenna systems can improve system performance and increase system capacity.

We also investigated the effect of K_d and traffic per channel (a_c) on the spectral efficiency for omnidirectional systems (Figure 4.11). We can say, for a fixed BER, increased values of K_d and a_c lead to higher spectral efficiencies. The effects of K_d and correlation coefficient between the signals (ρ), on the spectral efficiency were also compared for omnidirectional and 120° directional systems (Figure 4.12 and 4.13). When the signals are correlated, the directional antenna system is more successful than the uncorrelated case.

But adaptive antenna systems give the best results in terms of BER, when compared to the omnidirectional and directional antenna systems in all cases. An adaptive array of M antenna elements can suppress up to $M-1$ interferers. Computer simulations performed with Matlab* show four successful examples for this (Figure 5.4-5.7). In the simulation, a uniformly spaced 10-element linear adaptive array is under investigation. The signals coming to the array are under flat Rayleigh fading. We have equal-power (same SIR) interferers coming from different but known directions. By changing the number of interferers, the adaptive array's interference suppressing capability and error performance are analyzed. The array uses LMS (Least Mean Square) algorithm for adaptation. Convergence rate and mean squared error value are two important parameters in the computations. When the adaptation finishes, the adaptive array places its nulls to the directions of interference and its main beam to the desired signal direction in the radiation pattern.

Finally the effects of signal (channel) correlation, standard deviation of shadowing (σ), modulation method and number of the antenna elements (μ), on the PCI were investigated for 1-interferer and 6-interferer cases (Figure 6.2-6.7). Results show that; increasing μ will decrease both PCI and BER. The adaptive array performs better with correlated interferers than with uncorrelated interferers. Also obtained is the result showing, NCDPSK modulation is superior than NCFSK.

*: Matlab is a trademark of the Mathworks Inc.

REFERENCES

- [1]: Theodore S. RAPPAPORT, "Wireless Communications, Principles and Practice, 2nd Edition", Prentice Hall, 2002.
- [2]: William C.Y. LEE, "Elements of Cellular Mobile Radio Systems", IEEE Transactions on Vehicular Technology, vol.VT-35, pp.48-56, May 1986.
- [3]: William C.Y. LEE, "Smaller Cells for Greater Performance", IEEE Communications Magazine, November 1991.
- [4]: Aysel ŞAFAK, "Spectrum Efficiency in Cellular Mobile Radio Systems with Multiple Correlated Signals", Proceedings of 7th Mediterranean Electrotechnical Conference (MELECON' 94), vol.1, pp.137-140, 12-14 April 1994, Antalya, TURKEY.
- [5]: A. ŞAFAK, "Optimal Channel Reuse in Mobile Cellular Radio Systems with Multiple Correlated Log-normal Interferers", IEEE Transactions on Vehicular Technology, vol.VT-43,no.2, May1994.
- [6]: John LITVA, "Digital Beamforming in Wireless Communications", Artech House, 1996.
- [7]: Hirofumi SUZUKI, "A Statistical Model for Urban Radio Propagation", IEEE Transactions on Communications, vol. COM-25, no.7, pp.673-680, July 1977.
- [8]: Bernard SKLAR, "Rayleigh Fading Channels in Mobile Digital Communication Systems, Part I: Characterization", IEEE Communications Magazine, September 1997.
- [9]: Aysel ŞAFAK, "Statistical Analysis of the Power Sum of Multiple Correlated Log-normal Components", IEEE Transactions on Vehicular Technology, vol.VT-41, no.1, pp.58-61, February 1993.
- [10]: A. ŞAFAK and M. ŞAFAK, "Moments of the Sum of Correlated Log-normal Random Variables", Proceedings of the IEEE / VTS 44th Vehicular Technology Conference, 7-11 June 1994, Stockholm, SWEDEN.
- [11]: A. ŞAFAK, R.PRASAD and J.P.M.G. LINNARTZ, "Outage Probability Analysis for Mobile Radio Systems Due to Correlated Log-normal Interferers", Proceedings of the 1990 Bilkent International Conference on New Trends in Communication, Control, and Signal Processing, Ankara, TURKEY, pp.518-524, July 1990.
- [12]: A. ŞAFAK and R. PRASAD, "Effects of Correlated Shadowing Signals on Channel Reuse in Mobile Radio Systems", IEEE Transactions on Vehicular Technology, vol.40, no.4, pp.708-713, November 1991.

- [13]: G.K. Chan, "Effects of Sectorization on the Spectrum Efficiency of Cellular Radio Systems", IEEE Trans. Veh. Tech., vol.41, no.3, pp.217-225, August 1992.
- [14]: A. ŞAFAK, B. USLU, "Sektörize Hücreli İletişim Sistemlerinin Başarım Analizi", ELECO' 2000, Elektrik-Elektronik-Bilgisayar Mühendisliği Sempozyumu, 8-12 Kasım Bursa, TÜRKİYE.
- [15]: Jack SALZ, "Effect of Fading Correlation on Adaptive Arrays in Digital Mobile Radio", IEEE Transactions on Vehicular Technology, vol.43, no.4, pp.1049-1057, November 1994.
- [16]: Anders DERNERYD and Björn JOHANNISSON, "Adaptive Base Station Antenna Arrays", Ericsson Review No.3, 1999.
- [17]: Simon HAYKIN, "Adaptive Filter Theory", Wiley, 1996.
- [18]: George-Othon GLENTIS, Kostas BERBERIDIS, and Sergios THEODORIDIS, "Efficient Least Squares Adaptive Algorithms for FIR Transversal Filtering", IEEE Signal Processing Magazine, July 1999.
- [19]: Aysel ŞAFAK, Sertaç BAHADIR, Baran USLU, "Gezgin İletişim Sistemlerinde Adaptif Hüzmeşekillendirme", URSI-2002, 18-20 Eylül, İstanbul, TÜRKİYE.

Ö Z G E Ç M İ Ş

İ B R A H İ M B A R A N U S L U



Araştırma Görevlisi
Başkent Üniversitesi, Elektrik Elektronik Mühendisliği Bölümü

Eskişehir Yolu 20. km Bağlıca Kampüsü, Etimesgut 06530 / ANKARA
Tel: (0312) 234 1010 , Faks: (0312) 234 1051
E-posta: ibuslu@baskent.edu.tr

KİŞİSEL BİLGİLER

Doğum: 18.02.1976 Ankara

Medeni Durum: Bekar

ÇALIŞMA DENEYİMİ

03.2000-... Başkent Üniversitesi EEM Bölümü Ankara
Araştırma Görevlisi

02.1999-03.2000 Hacettepe Üniversitesi EEM Bölümü Ankara
Araştırma Görevlisi

EĞİTİM

03.2000 – 01.2003 Başkent Üniversitesi
■ Yüksek Lisans, Elektrik -Elektronik Mühendisliği
Genel Ortalama: 3.4/4.0

09.1994 – 09.1998 Ankara Üniversitesi
■ Lisans, Elektronik Mühendisliği
Genel Ortalama: 75.6/100

10.1991- 06.1994 Özel Arı Fen Lisesi (Burslu)
Genel Ortalama: 4.91/5.00